Adaptive observations in 4D-Var data assimilation

I.M. NAVON
Department of Mathematics and
School of Computational Science
Florida State University,
Tallahassee,Florida 32306-4120

LECTURE PLAN

- Introduction
- The S-W equations model
- Targeting strategies
- 4-D Var data assimilation and adaptive observations
- SVD approach
- Gradient sensitivity approach
- Interaction between adaptive observations
- Weighting the interaction between observations
- Numerical results
- Summary and future work

Introduction

The forecast of some severe meteorological events (e.g. hurricane) is a difficult prediction problem even at short range (12 to 48 hours).

Small but fast-growing initial errors may lead to significant uncertainties in forecasts and severe forecast failures with dramatic consequences in terms of societal impact.

Short term prediction of rapidly evolving meteorological events may be greatly improved by reducing analysis errors in dynamically sensitive geographical regions.

Adaptive (or "targeted") observations are atmospheric data which are obtained in certain areas that are believed to be critical for improvements to initial conditions used in numerical weather prediction models.

Targeted observations strategies must account for uncertainty magnitude, uncertainty growth *and* the details of the data assimilation scheme.

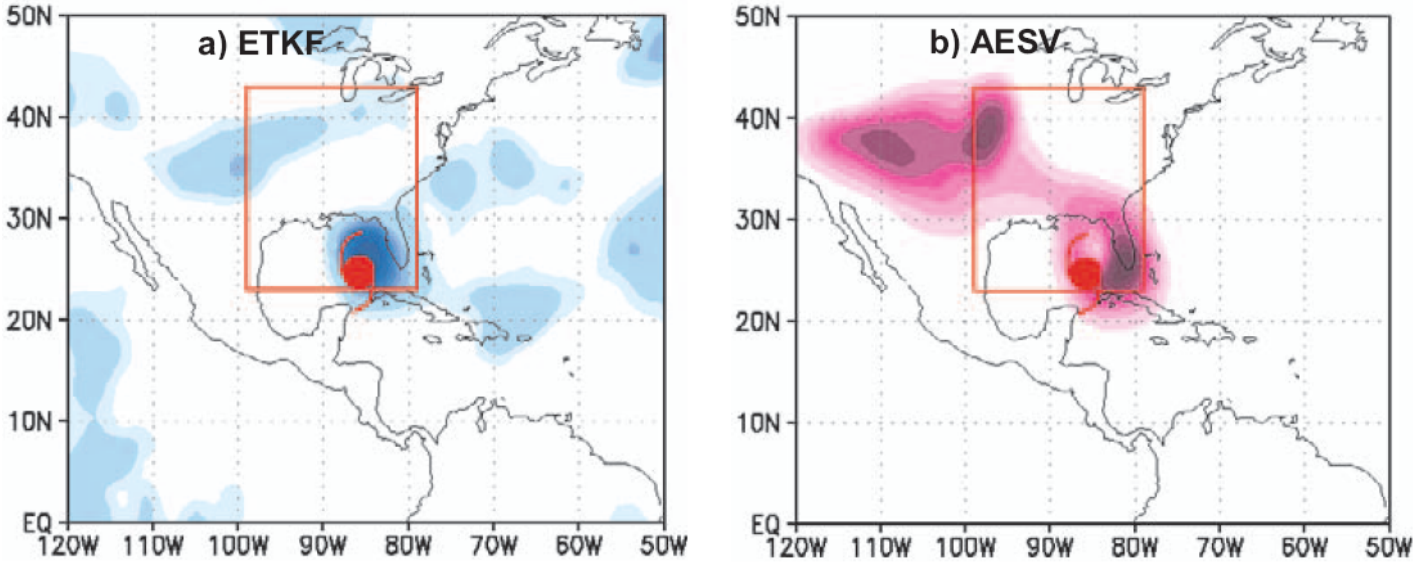

Figure 1. Targeting guidance at 00 UTC 28 August 2005 in a 48 h forecast of Hurricane Katrina: (a) from the ensemble-transform Kalman Filter, with 20 NCEP ensemble members; (b) from analysis-error singular vectors (SVs) of the Navy Operational Global Atmospheric Prediction System (NOGAPS), shown as vertically integrated total energy weighted by growth rate (singular value), summed for the three fastest growing SVs. The forecast verification region in the targeting calculations is within the red solid lines, based on the anticipated forecast position of Katrina at 00 UTC 30 August 2005. The targeting guidance is produced using forecast fields from initial conditions at 00 UTC 26 August 2005 (48 h prior to the targeted observing time). The position of Katrina at the targeted observing time is indicated by the red hurricane symbol. Colour shading indicates potential areas for the addition of targeted observations. See text for further details. (Illustration provided by S. Majumdar (a) and C. Reynolds (b).)

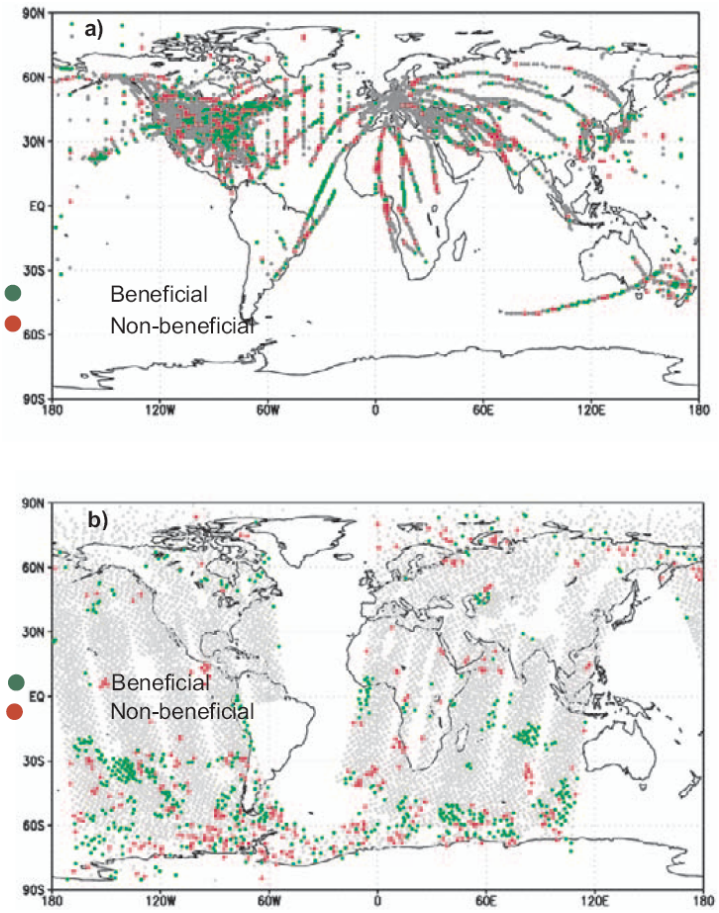

Figure 2. Impact of: (a) commercial aircraft temperature and wind observations, and (b) Advanced Microwave Sounding Unit (AMSU)-A channel-6 brightness temperature (radiance) observations, assimilated in NAVDAS, using 3D-Var, at 00 UTC 28 February 2005. Green dots mark the locations of observations that produce negative (beneficial) values of $\mathbf{e}_{24} - \mathbf{e}_{30}$, which is a measure of energy-weighted forecast error in the global domain; $\mathbf{e}_{24}$ is the 24 h forecast error on the 'analysis trajectory', which starts from an analysis at 00 UTC 28 February 2005, and $\mathbf{e}_{30}$ is the 30 h forecast error on the 'background trajectory,' which starts from an analysis at 18 UTC 27 February 2005. Red dots are locations of observations that are non-beneficial in this forecast measure. If $\mathbf{e}_{24} - \mathbf{e}_{30} < 0$ for a specific observation, or set of observations, then the assimilation of those observations has produced a more accurate forecast trajectory, in terms of the global measure of forecast error. Grey dots indicate relatively small negative or positive observation impact. The methodology of this calculation is described in Langland and Baker (2004b). See text for further details.

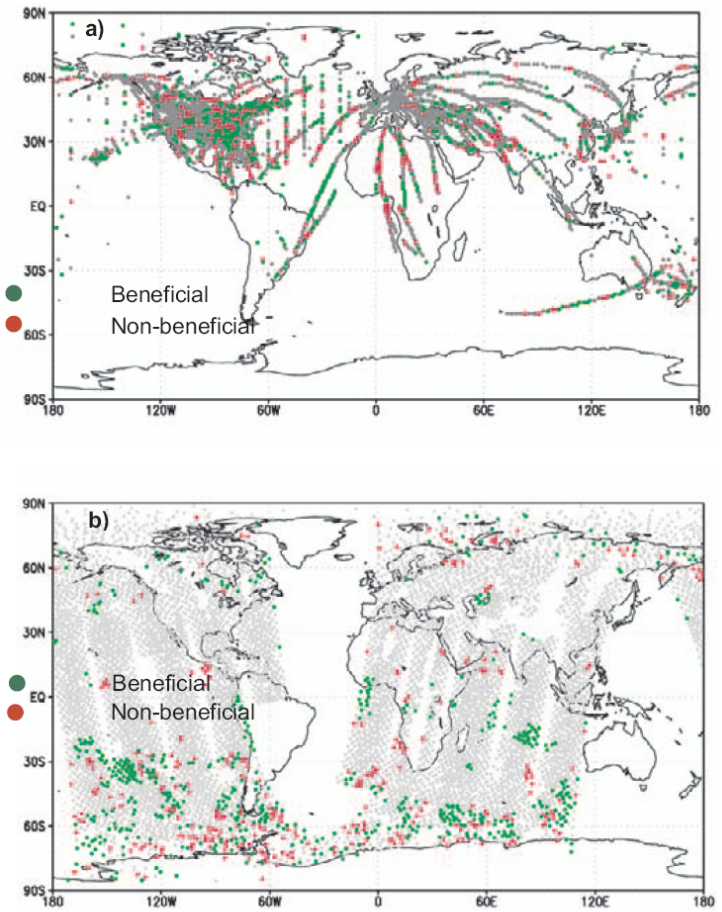

Figure 2. Impact of: (a) commercial aircraft temperature and wind observations, and (b) Advanced Microwave Sounding Unit (AMSU)-A channel-6 brightness temperature (radiance) observations, assimilated in NAVDAS, using 3D-Var, at 00 UTC 28 February 2005. Green dots mark the locations of observations that produce negative (beneficial) values of $\mathbf{e}_{24} - \mathbf{e}_{30}$, which is a measure of energy-weighted forecast error in the global domain; $\mathbf{e}_{24}$ is the 24 h forecast error on the 'analysis trajectory', which starts from an analysis at 00 UTC 28 February 2005, and $\mathbf{e}_{30}$ is the 30 h forecast error on the 'background trajectory,' which starts from an analysis at 18 UTC 27 February 2005. Red dots are locations of observations that are non-beneficial in this forecast measure. If $\mathbf{e}_{24} - \mathbf{e}_{30} < 0$ for a specific observation, or set of observations, then the assimilation of those observations has produced a more accurate forecast trajectory, in terms of the global measure of forecast error. Grey dots indicate relatively small negative or positive observation impact. The methodology of this calculation is described in Langland and Baker (2004b). See text for further details.

The shallow water model equations

The shallow water equations in spherical coordinates are given by

$$\frac{\partial u}{\partial t} + \frac{1}{a\cos\theta}\left[u\frac{\partial u}{\partial \lambda} + v\cos\theta\frac{\partial u}{\partial \theta}\right] - (f + \frac{u}{a}\tan\theta)v + \frac{g}{a\cos\theta}\frac{\partial h}{\partial \lambda} = 0 \quad (1)$$

$$\frac{\partial v}{\partial t} + \frac{1}{a\cos\theta}\left[u\frac{\partial v}{\partial \lambda} + v\cos\theta\frac{\partial v}{\partial \theta}\right] + (f + \frac{u}{a}\tan\theta)u + \frac{g}{a}\frac{\partial h}{\partial \theta} = 0 \quad (2)$$

$$\frac{\partial h}{\partial t} + \frac{1}{a\cos\theta}\left[\frac{\partial}{\partial \lambda}(hu) + \frac{\partial}{\partial \theta}(hv\cos\theta)\right] = 0 \quad (3)$$

where $f = 2\Omega\sin\theta$ is the Coriolis parameter, Ω is the angular speed of the rotation of the earth, h is the height of the homogeneous atmosphere, u and v are the zonal and meridional wind components respectively, θ and λ are the latitudinal and longitudinal directions respectively, a is the radius of the earth, and g is the gravitational constant.

Model Discretization

The model is integrated for 24h on a 72×36 grid ($5^\circ \times 5^\circ$) using an explicit Turkel-Zwas scheme (Neta et al., JCP 1997) with a time step $\Delta t = 200s$.

A Robert fitering using a Laplacian type time-diffusion term is performed for both spatial and temporal smoothing.

The dimension of the discrete state vector $\mathbf{x} = (h, u, v)$ is 7776.

Data from NASA $500mb$ analysis valid for 00Z 16 Mar 2001 6hr with a model resolution of 1 degree by 1.25 degrees using the GEOS-3 model, is used to specify the geopotential height at the initial time t_0 and the velocities at t_0 are obtained from a geostrophic approximation.

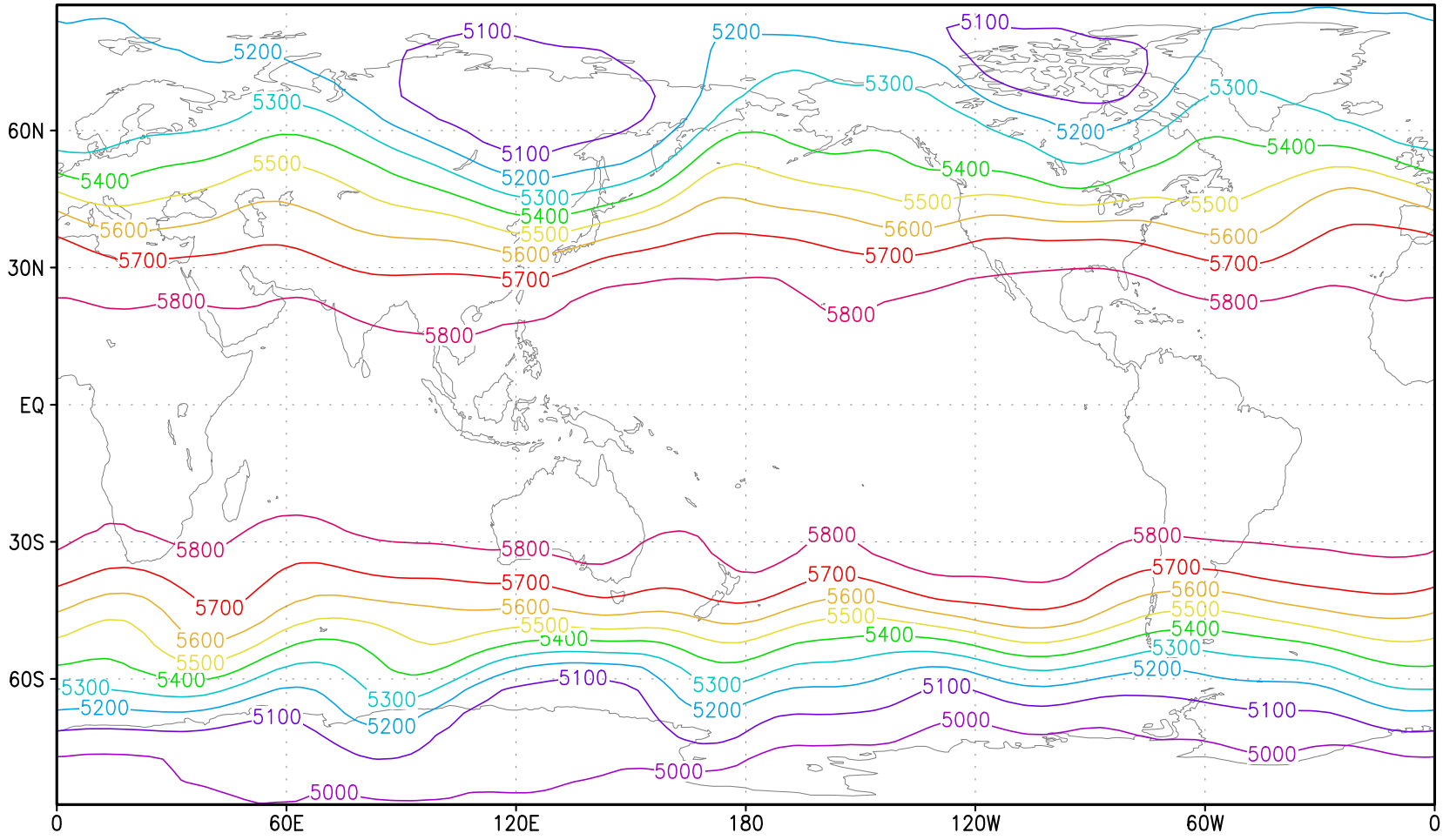
500hPa geopotential height at t=24h
60N
30N
EQ
30S
60S
0
60E
120E
180
120W
60W
0
5100
5200
5300
5400
5500
5600
5700
5800
5000

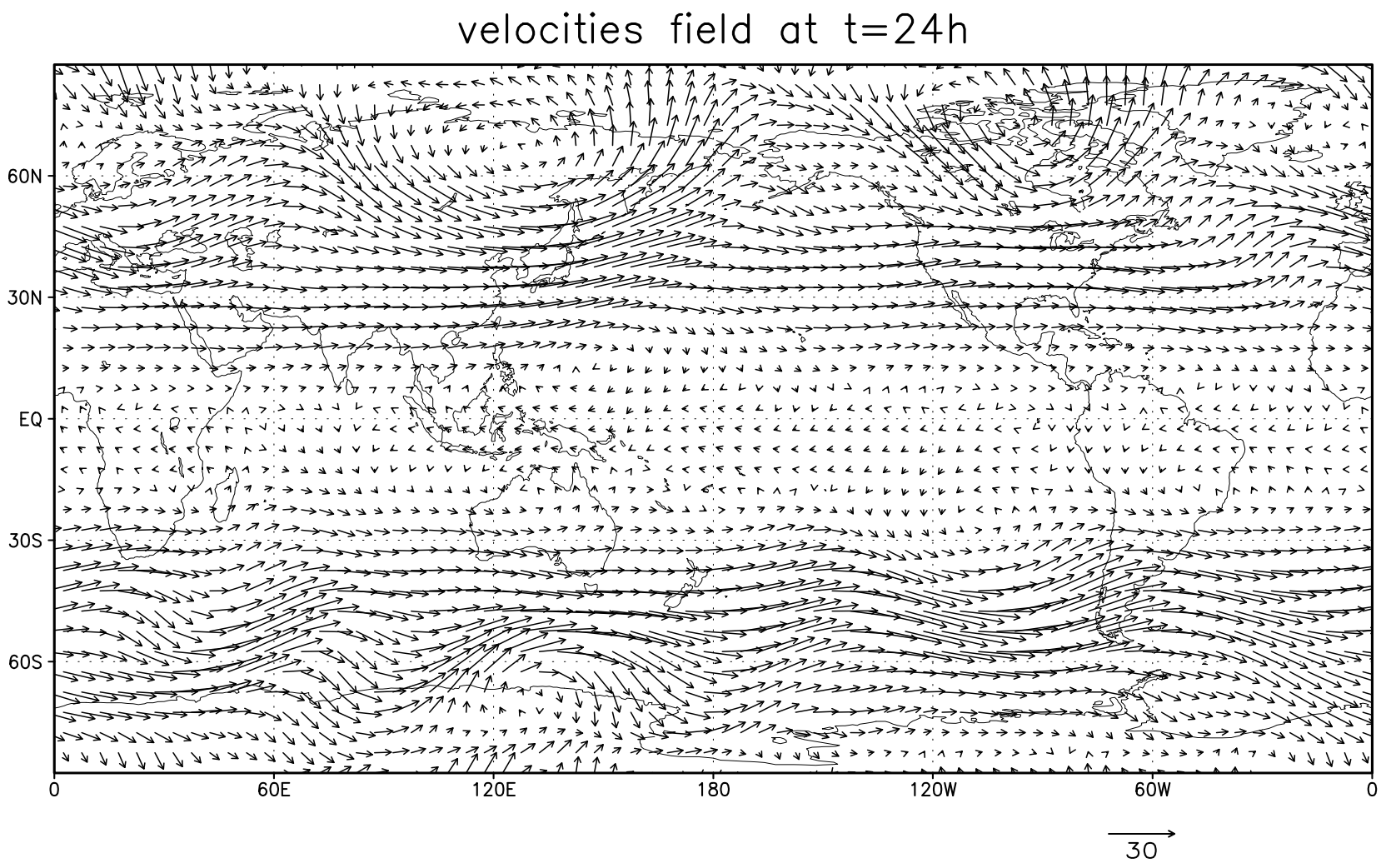
velocities field at t=24h
60N
30N
EQ
30S
60S
0
60E
120E
180
120W
60W
0
30

500hPa geopotential height at t=0h

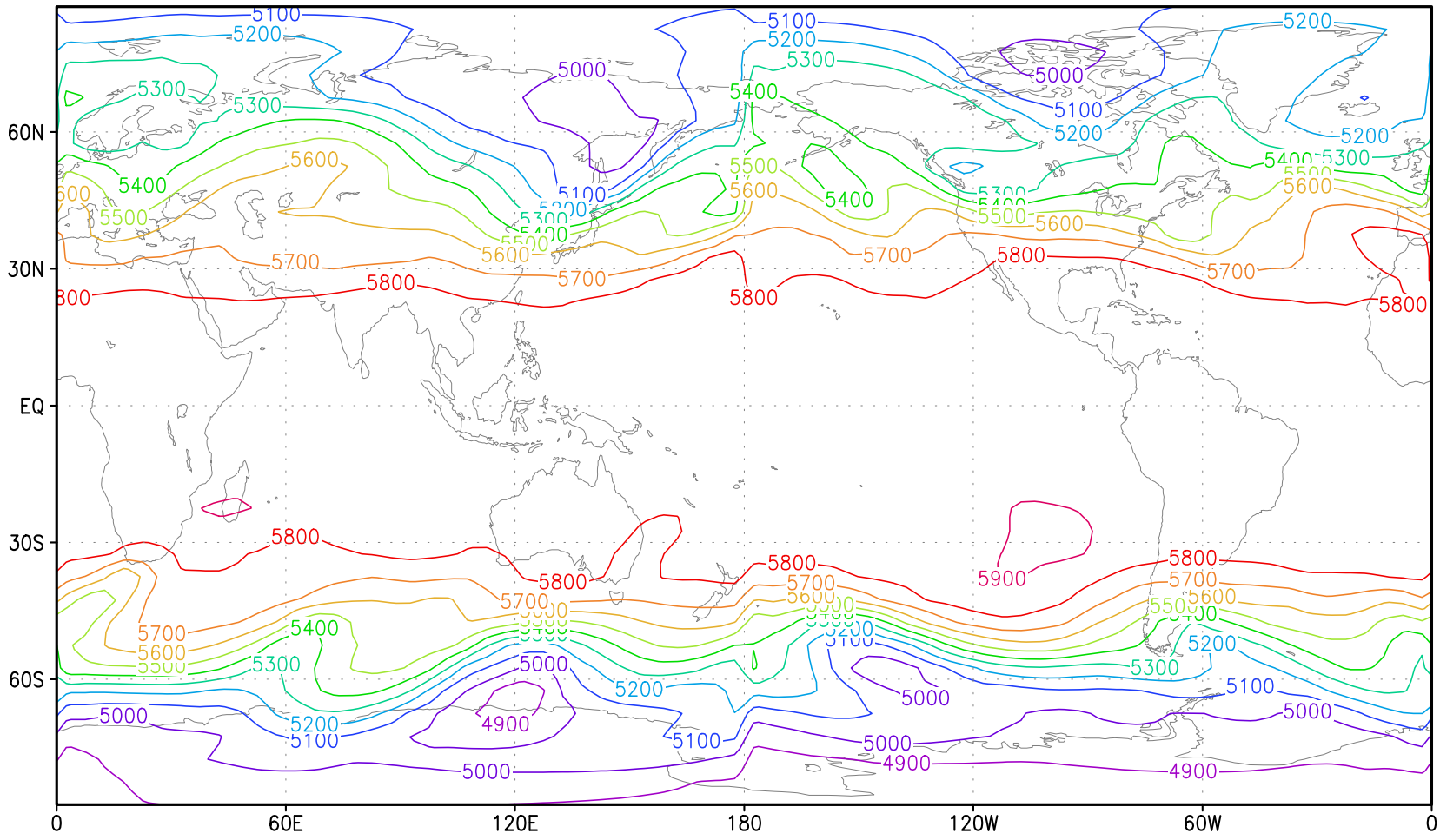

velocities field at initial time t=0h

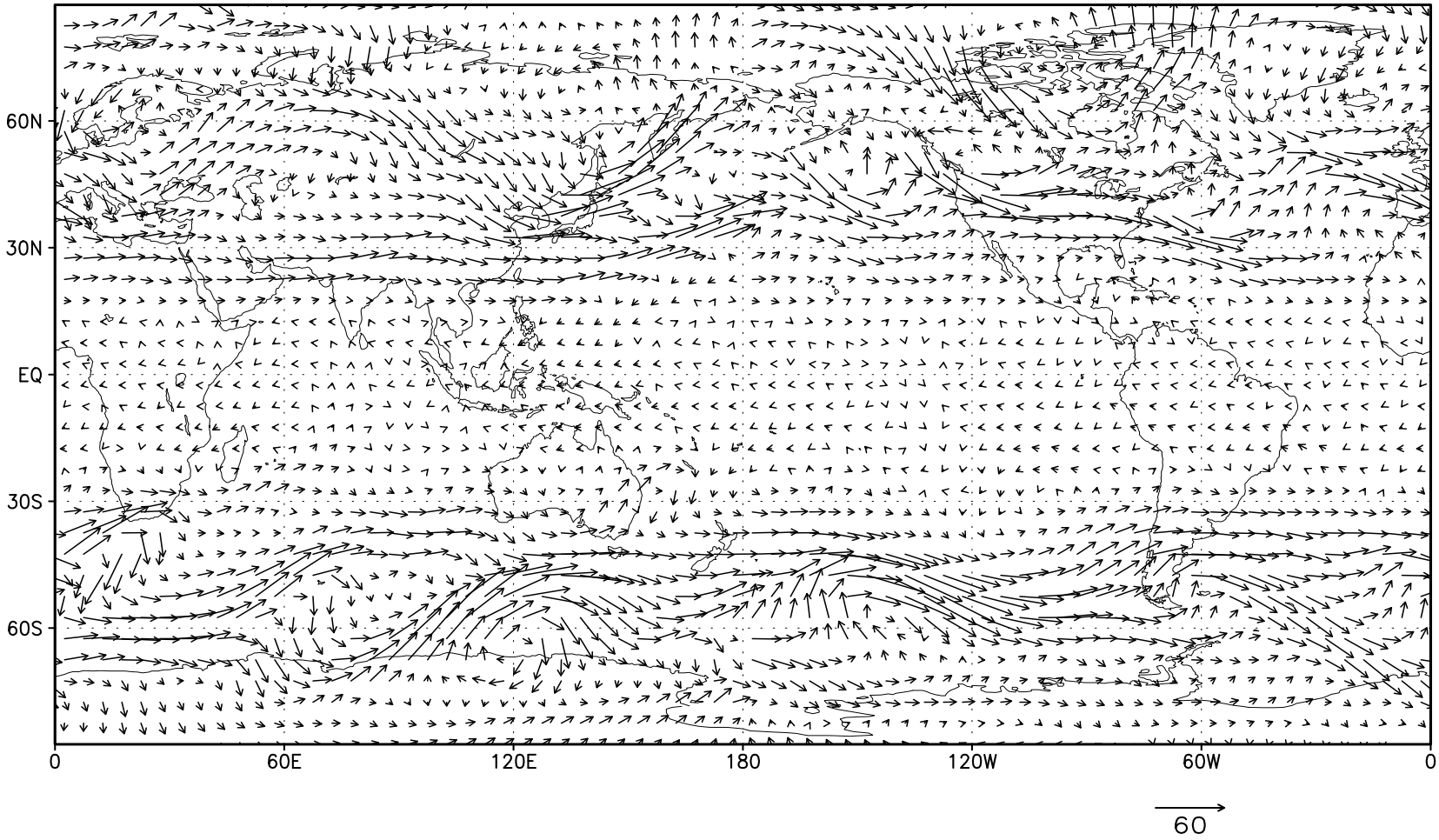

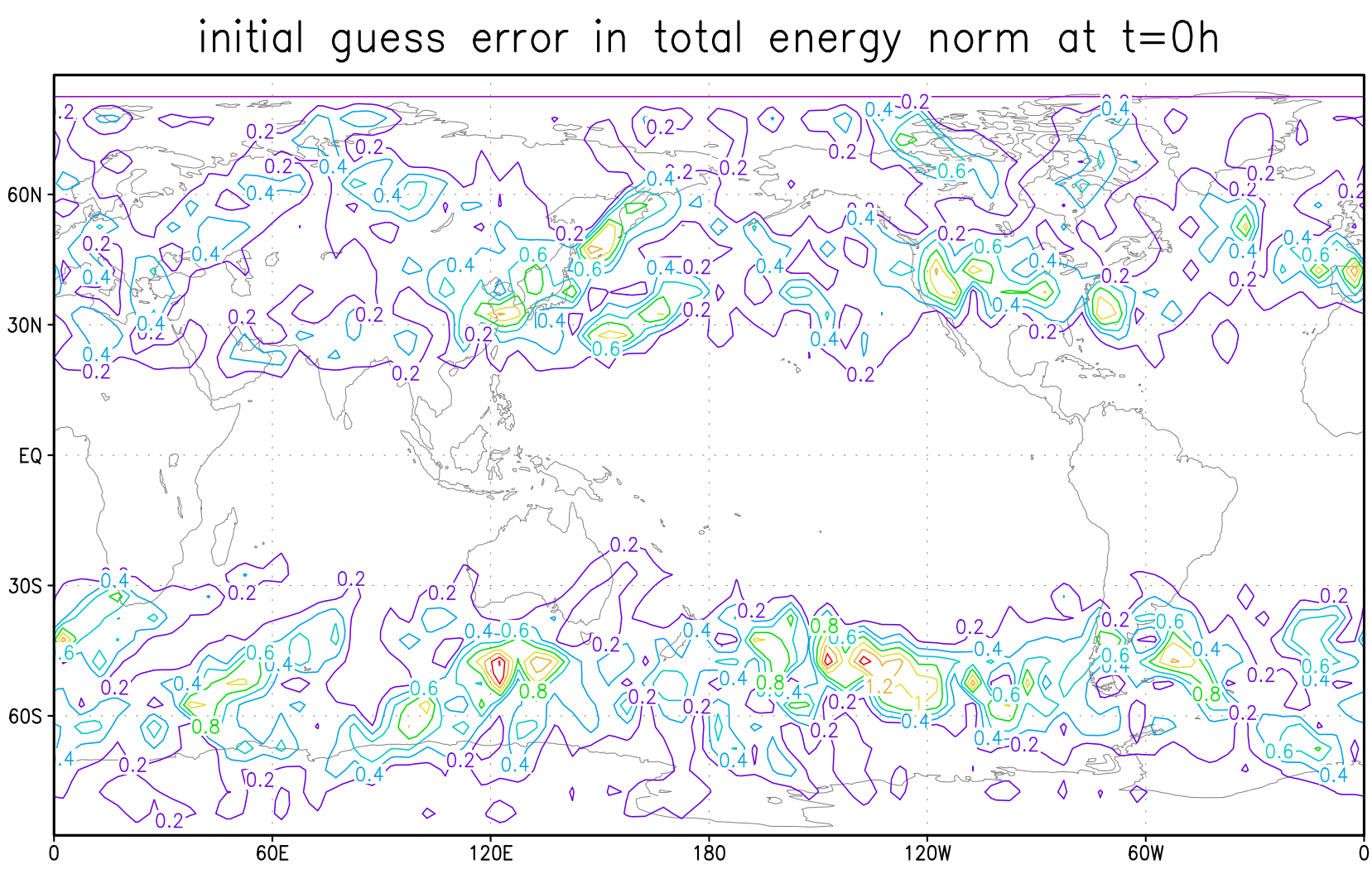
initial guess error in total energy norm at t=0h
60N
30N
EQ
30S
60S
0
60E
120E
180
120W
60W
0

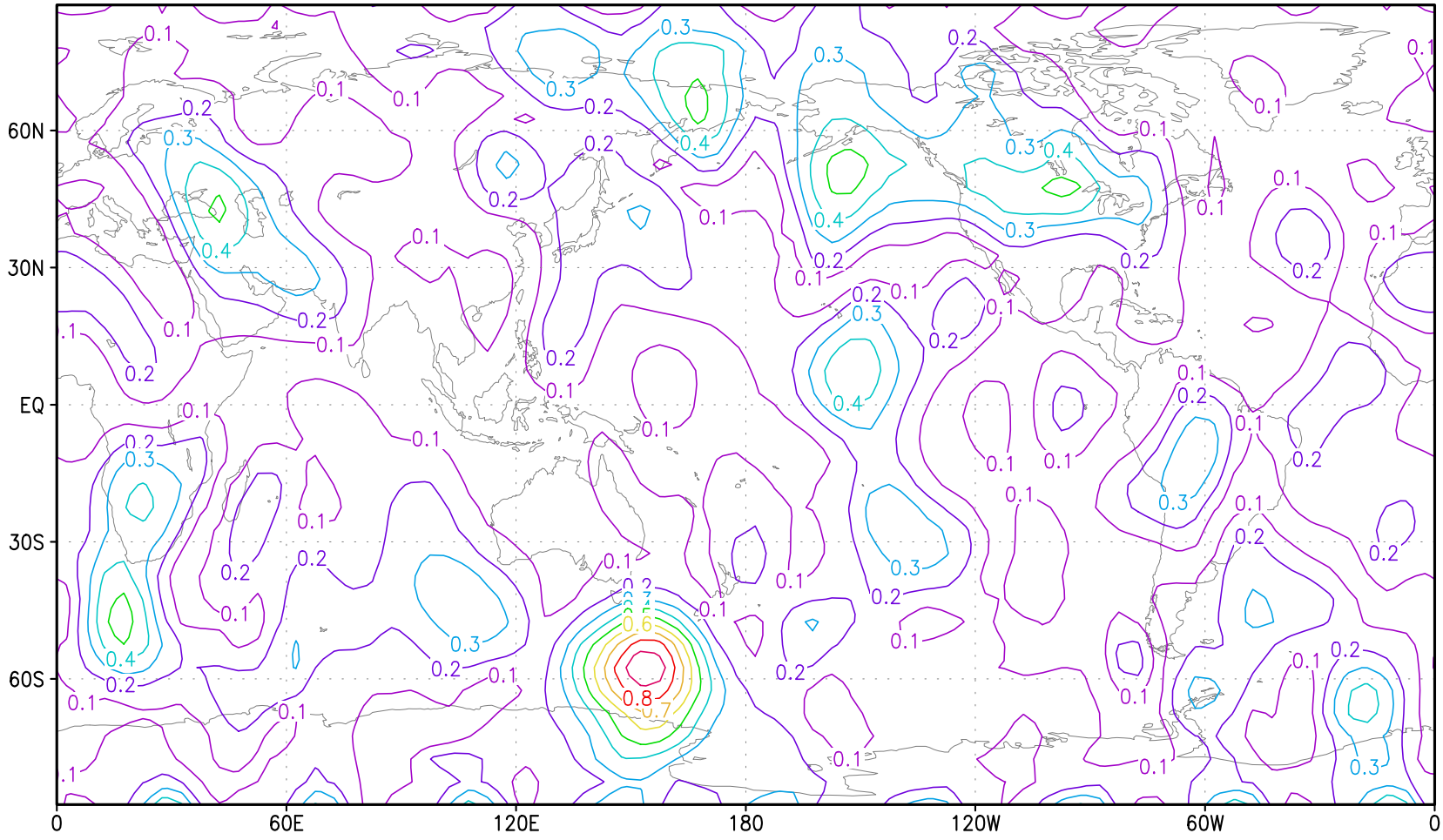
initial guess error in total energy norm at t=24h
60N
30N
EQ
30S
60S
0
60E
120E
180
120W
60W
0

error (t.e. norm) of 24h forecast with fixed obs only

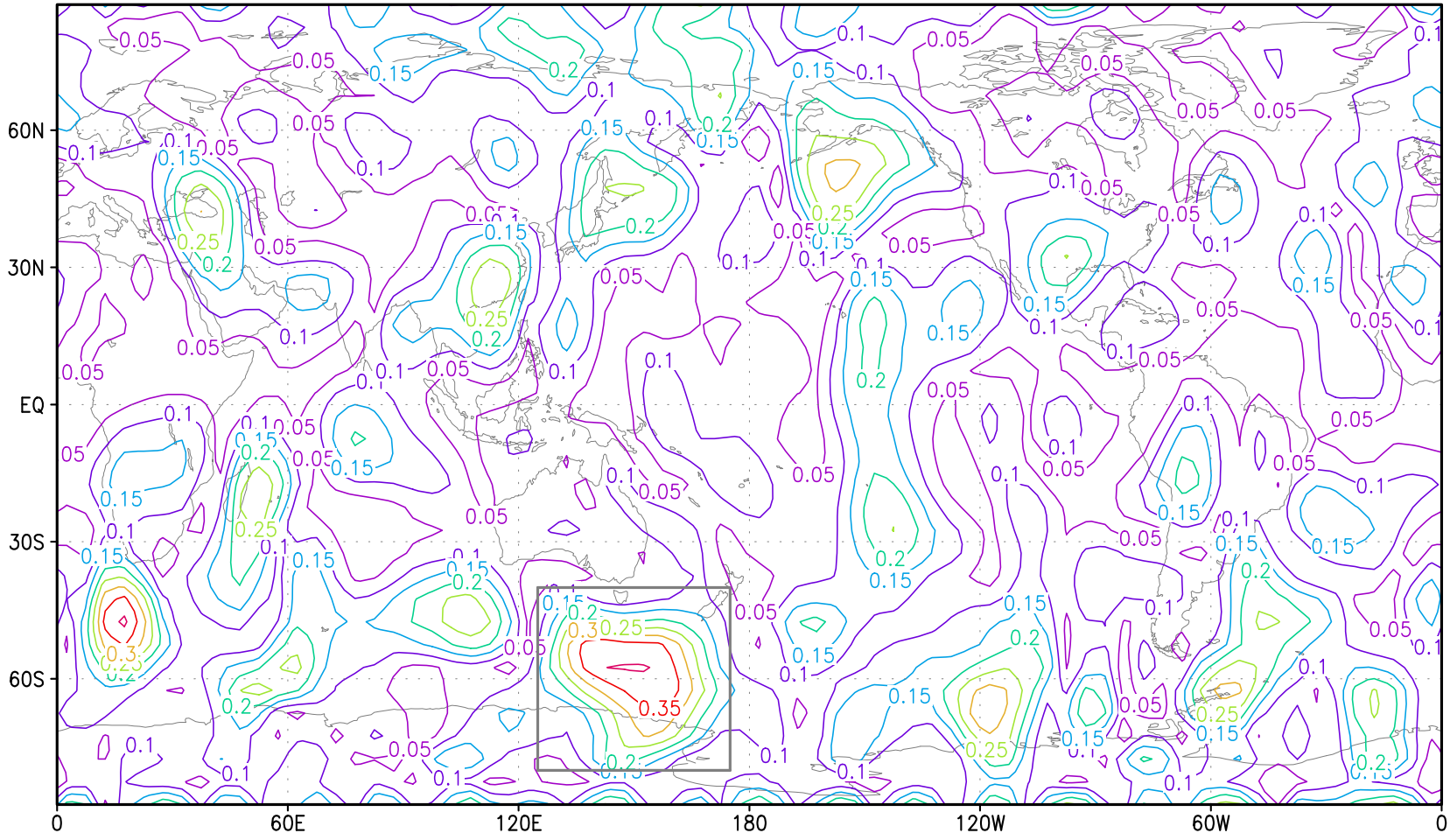

The adaptive (targeted) observations procedure involves three time levels (Szunyogh et al., MWR 2002):

- In the first step, a potentially severe weather event is selected at planning time t_0 based on the latest forecast products
- A future verification time $t_v > t_0$ and a verification domain $\mathcal{D}_v$ for the event are chosen accordingly
- A sensitivity analysis is then performed to determine the *future observational time* $t_0 < t^o < t_v$ and observational region (target area) $\mathcal{D}^o$ where additional observations taken at t^o are most likely to significantly reduce the forecast error of the selected weather event at t_v.

Current targeting programs use only one targeting time t^o and a sequential data assimilation procedure (Majumdar et al., MWR 2001).

In the 4D-Var data assimilation context, optimal deployments of supplementary observations on a time-varying domain $\mathcal{D}_i^o$ must be determined for a sequence of intervening times $t_0 < t_1^o < \ldots < t_I^o < t_v$.

Targeting strategies

Current targeting strategies include

1. *Singular vector technique* (Palmer et al., Gelaro et al., JAS 1998)
2. *Gradient sensitivity technique* (Langland et al., QJRMS 1999)
3. Observation sensitivity technique (Baker and Daley, QJRMS 2000)
4. Quasi-linear model technique (Pu and Kalnay, QJRMS 1999)
5. Ensemble transform technique (Bishop and Toth, JAS 1999)
6. Ensemble transform Kalman Filter (Bishop et al., MWR 2001)

In what follows we will consider SV and gradient sensitivity techniques in the 4D-Var context.

Field experiments (THORPEX, FASTEX, NORPEX, WSRP) revealed that the efficiency of adaptive observations is influenced by the data assimilation scheme employed.

The design of the adaptive observations strategies must take into account the particular properties of the data assimilation method (Bergot QJRMS, 2001).

4D-Var Data Assimilation and Adaptive Observations

Observational data in the analysis time interval $[t_0, T], T < t_v$ has two components

$\mathcal{O}^f$ - set of observations provided by the routine observational network which location is 'a priori' known at t_0 (Superscript f is for fixed).

$\mathcal{O}^a$ - set of adaptive observations selected according to an optimality criteria

$$\mathcal{O}^a = \{\mathcal{O}^a_1, \mathcal{O}^a_2, \ldots \mathcal{O}^a_I\}$$

Minimization of the cost functional

$$\begin{aligned} \mathcal{J}(\mathbf{x}_0) &= \tfrac{1}{2}(\mathbf{x}_0 - \mathbf{x}^b)^T \mathbf{B}^{-1}(\mathbf{x}_0 - \mathbf{x}^b) \\ &+ \tfrac{1}{2}\sum_{k=0}^{m}(\mathbf{H}_k\mathbf{x}_k - \mathbf{x}^o_k)^T \mathbf{R}^{-1}_k(\mathbf{H}_k\mathbf{x}_k - \mathbf{x}^o_k) \end{aligned} \tag{4}$$

where $\mathbf{H}_k$ is a transformation matrix that maps the model variables to the

observation, $\mathbf{R}_k$ and $\mathbf{B}$ represent the covariance matrix of the observation errors and the background errors respectively, provides an optimal estimate $\mathbf{x}_0^\star : \mathcal{J}(\mathbf{x}_0^\star) = \min_{\mathbf{x}_0} \mathcal{J}(\mathbf{x}_0)$

Forecast error at t_v

$$\mathcal{J}_v(\mathbf{x}_0) = \frac{1}{2}\langle \mathbf{P}(\mathbf{x}_v - \mathbf{x}_v^{ref}), \mathbf{P}(\mathbf{x}_v - \mathbf{x}_v^{ref})\rangle_C \tag{5}$$

where $\mathbf{x}_v = M(\mathbf{x}_0)$, $\mathbf{x}_v^{ref}$ - verifying analysis at t_v, $\mathbf{P}$ - diagonal projection operator on $\mathcal{D}_v$, $\mathbf{P}^*\mathbf{P} = \mathbf{P}^2 = \mathbf{P}$, and the inner product $\langle \cdot, \cdot \rangle_C$ is defined by the total energy norm.

Assume that n_i additional observational resources may be deployed at each instant $t_i, i = 1, 2, \ldots I$.

Adaptive observations problem

Select a feasible observational path

$$\mathcal{O}^a = \{\mathcal{O}_1^a, \mathcal{O}_2^a, \ldots \mathcal{O}_I^a\}, \overline{\mathcal{O}}_i^a = n_i \tag{6}$$

such that $\mathcal{J}_v(\mathbf{x}_0^\star)$ is minimal.

Singular vectors approach (Buizza and Montani, JAS 1999)

Forecast model

$$\frac{d\mathbf{x}}{dt} = M(\mathbf{x}) \tag{7}$$

Tangent-linear model

$$\frac{d\delta\mathbf{x}}{dt} = \mathbf{M}(\mathbf{x})\delta\mathbf{x} \Rightarrow \delta\mathbf{x}(t) = \mathbf{L}(t_i, t)\delta\mathbf{x}(t_i) \tag{8}$$

where $\mathbf{L}(t_i, t)$ is the tangent forward propagator and $t - t_i$ is the optimization interval.

Consider an inner product on the tangent phase space

$$\langle \delta\mathbf{x}, \delta\mathbf{y} \rangle_C = \langle \delta\mathbf{x}, \mathbf{C}\delta\mathbf{y} \rangle \tag{9}$$

where $\mathbf{C}$ is a symmetric positive definite matrix (usually taken to be diagonal), and $\langle \cdot, \cdot \rangle$ the Euclidean inner product.

The adjoint operator of $\mathbf{L}$ in $\langle \cdot, \cdot \rangle_C$ is defined as:

$$\langle \mathbf{L}^{*C}\delta\mathbf{x}, \delta\mathbf{y} \rangle_C = \langle \delta\mathbf{x}, \mathbf{L}\delta\mathbf{y} \rangle_C \tag{10}$$

such that $\mathbf{L}^{*C} = \mathbf{C}^{-1}\mathbf{L}^{*}\mathbf{C}$.

It follows that

$$\|\delta\mathbf{x}(t)\|_C = \langle \delta\mathbf{x}(t_i), \mathbf{L}^{*C}\mathbf{L}\delta\mathbf{x}(t_i) \rangle_C \tag{11}$$

and the directions characterized by maximum growth $\|\delta\mathbf{x}(t)\|_C / \|\delta\mathbf{x}(t_i)\|_C$ are the singular vectors $\nu_j(t_i)$

$$\mathbf{L}^{*C}\mathbf{L}\nu_j(t_i) = \sigma_j^2 \nu_j(t_i) \tag{12}$$

associated with the largest singular values σ_j.

If $\mathbf{P}$ denotes the projection operator on $\mathcal{D}_v$, the singular value problem

$$\left[\mathbf{C}^{\frac{1}{2}}\mathbf{PLC}^{-\frac{1}{2}}\right]^{*}\mathbf{C}^{\frac{1}{2}}\mathbf{PLC}^{-\frac{1}{2}}\mu_j = \sigma^2\mu_j \tag{13}$$

$$\nu_j = \mathbf{C}^{-\frac{1}{2}}\mu_j \tag{14}$$

must be solved in the optimization interval $t_v - t_i$ for each $t_i, i = 1, 2, \ldots I$.

(!) Computationally expensive !

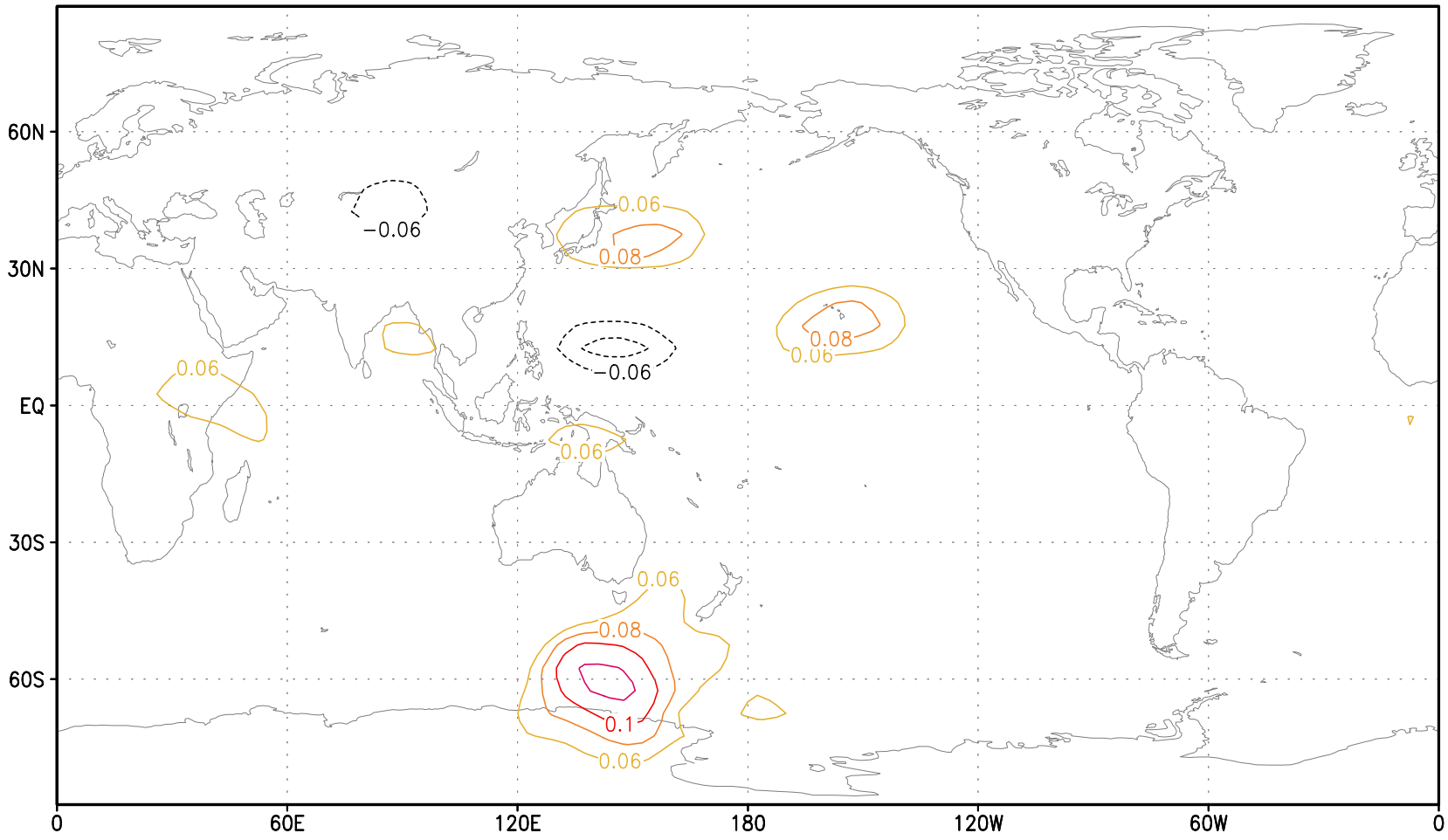
1st SV in 500hPa geopotential height field, [4,24]h
60N
30N
EQ
30S
60S
0
60E
120E
180
120W
60W
0
−0.06
0.06
0.08
−0.06
0.08
0.06
0.06
0.06
0.08
0.1
0.06

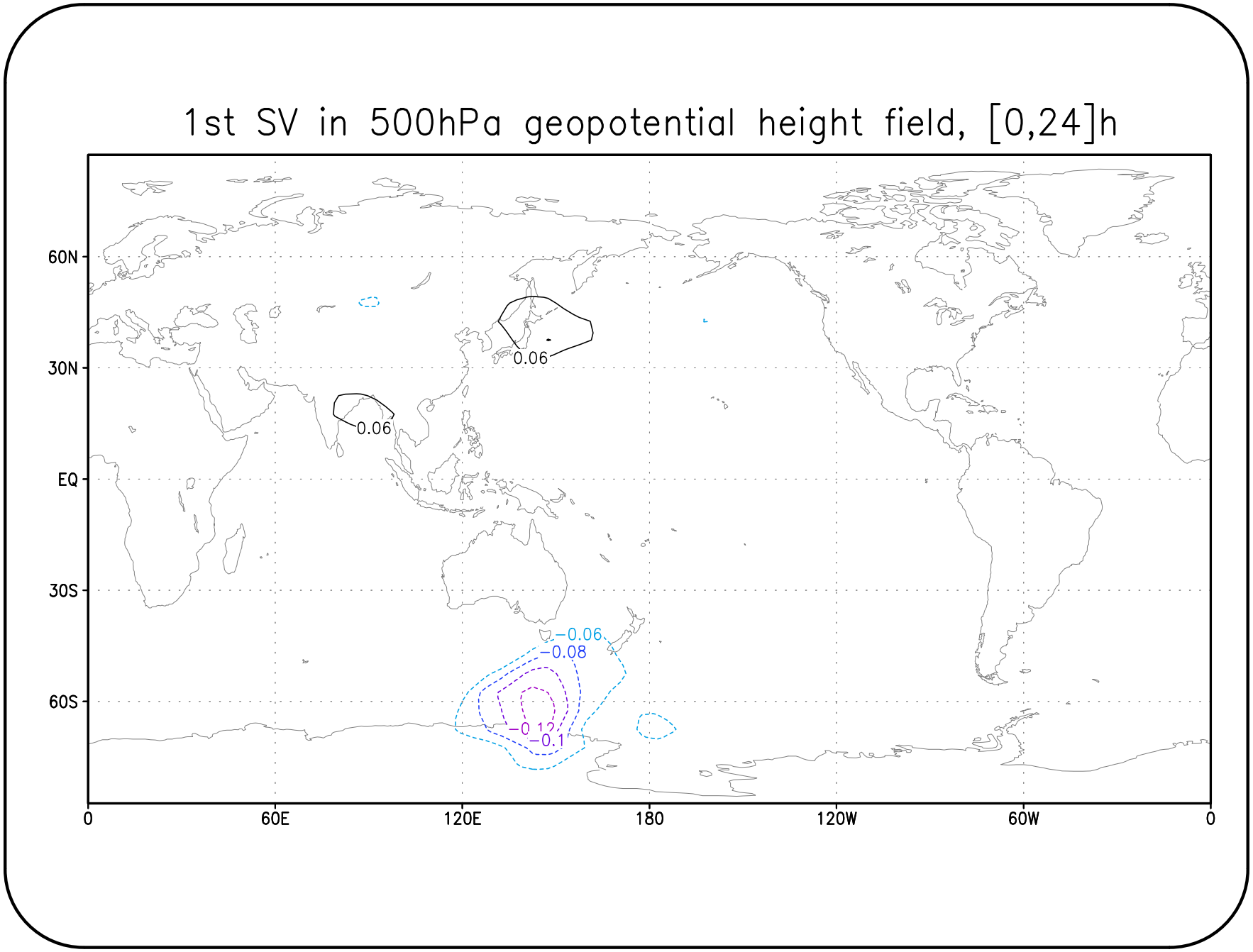
1st SV in 500hPa geopotential height field, [0,24]h
60N
30N
EQ
30S
60S
0
60E
120E
180
120W
60W
0
0.06
0.06
−0.06
−0.08
−0.12
−0.1

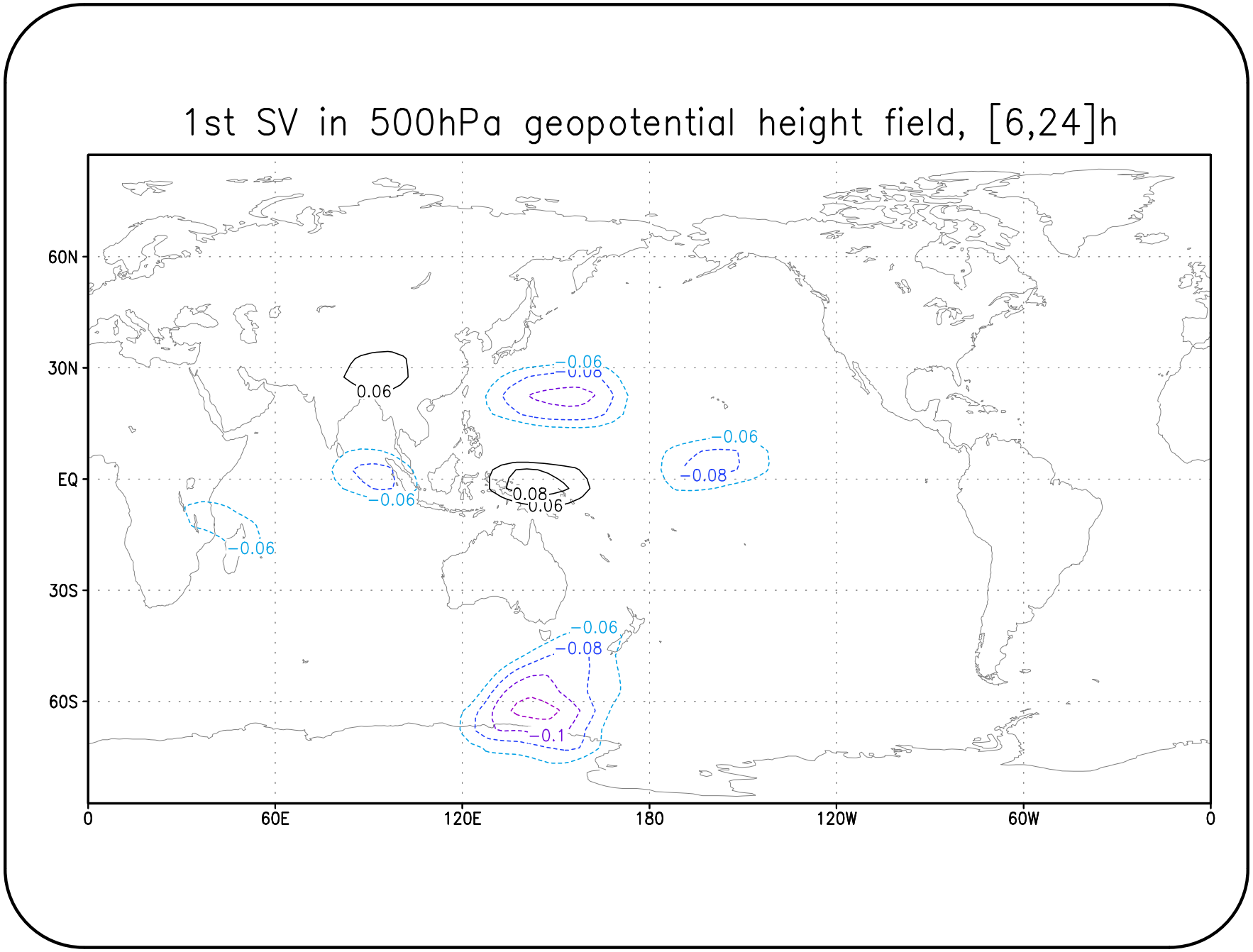
1st SV in 500hPa geopotential height field, [6,24]h
60N
30N
EQ
30S
60S
0
60E
120E
180
120W
60W
0
0.06
−0.06
−0.08
−0.1

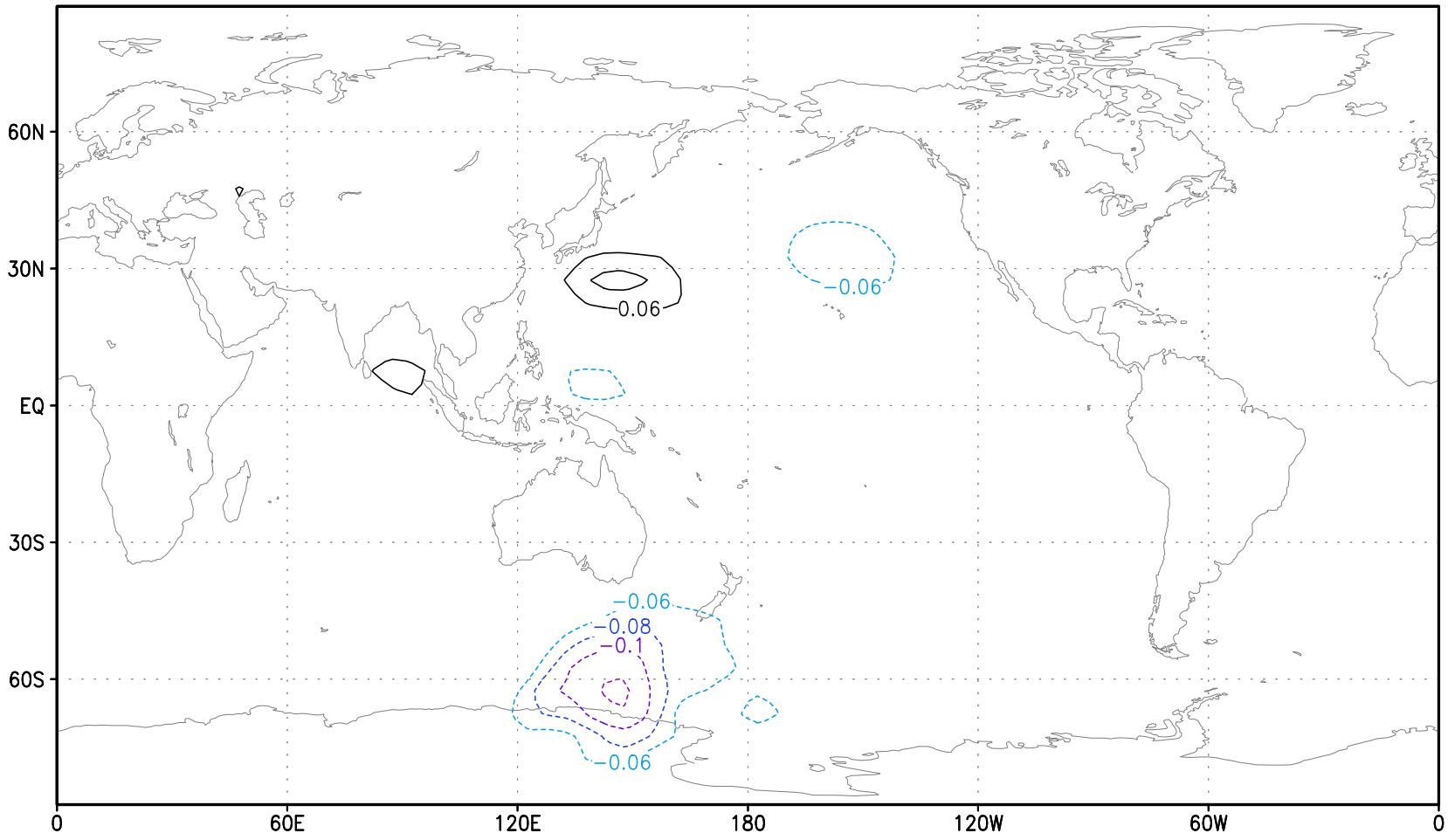
1st SV in 500hPa geopotential height field, [2,24]h
60N
30N
EQ
30S
60S
0
60E
120E
180
120W
60W
0
0.06
−0.06
−0.06
−0.08
−0.1
−0.06

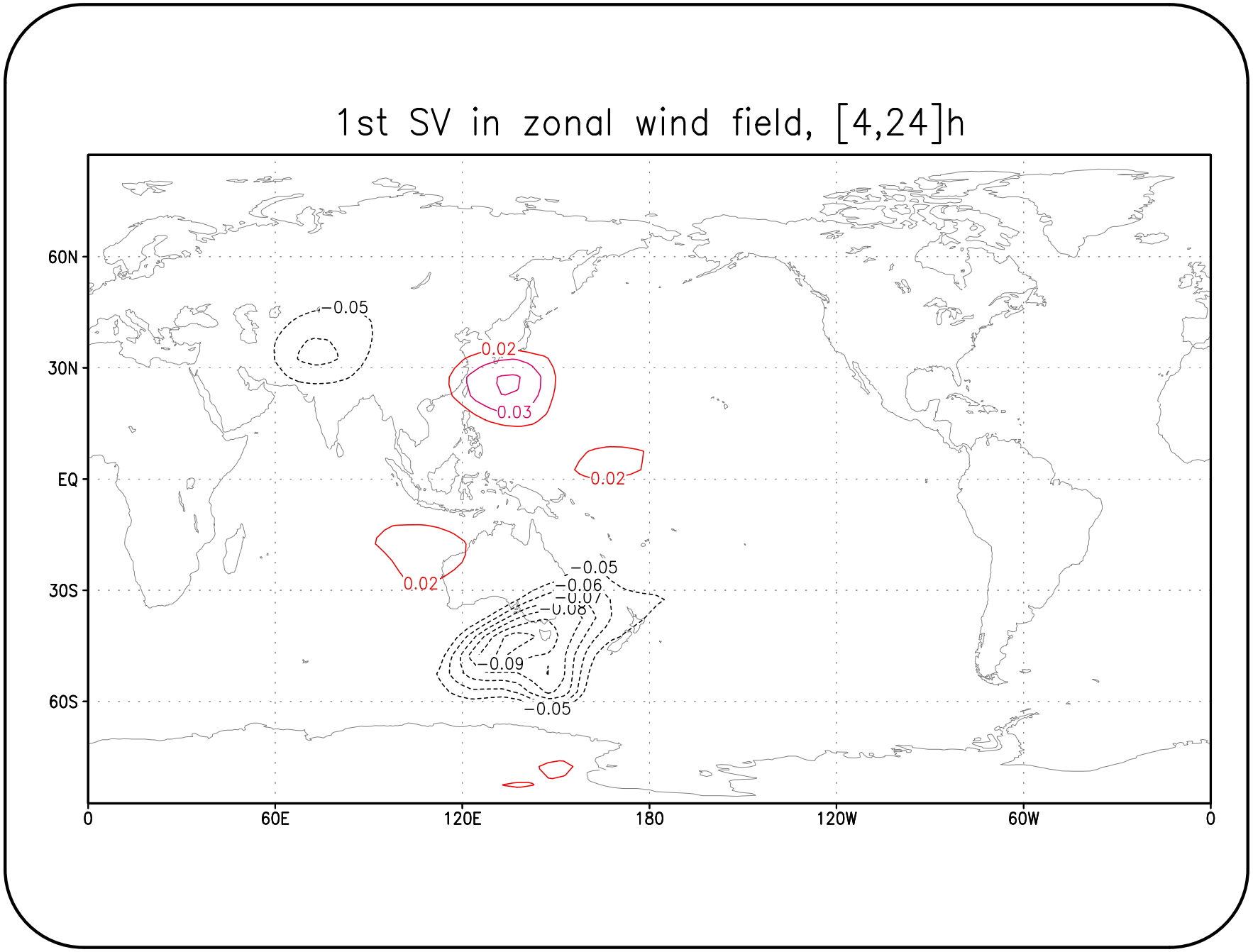
1st SV in zonal wind field, [4,24]h
60N
30N
EQ
30S
60S
0
60E
120E
180
120W
60W
0
−0.05
0.02
0.03
0.02
0.02
−0.05
−0.06
−0.07
−0.08
−0.09
−0.05

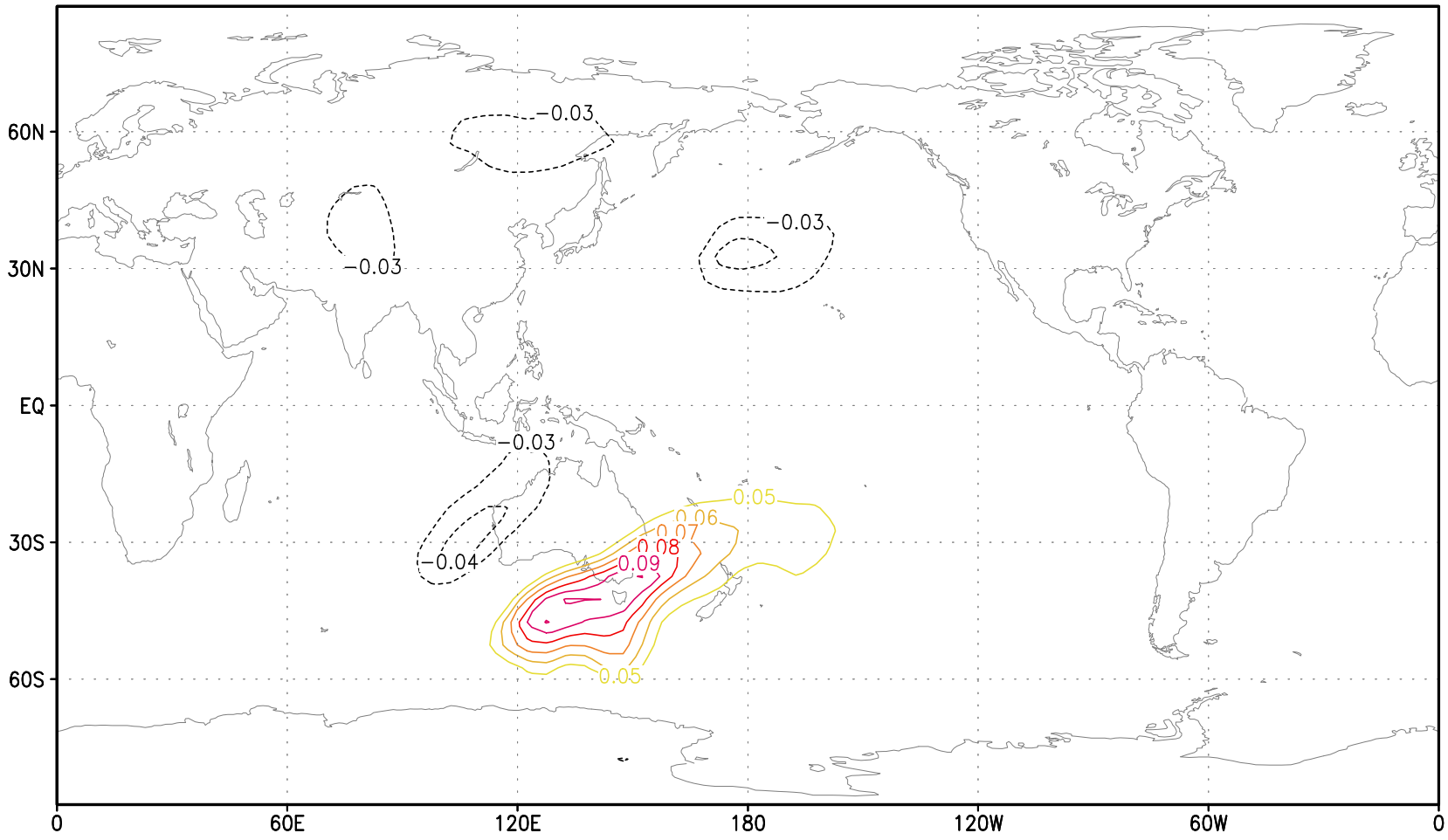
1st SV in zonal wind field, [0,24]h
60N
30N
EQ
30S
60S
0
60E
120E
180
120W
60W
0
−0.03
−0.03
−0.03
−0.03
−0.04
0.05
0.06
0.07
0.08
0.09
0.05

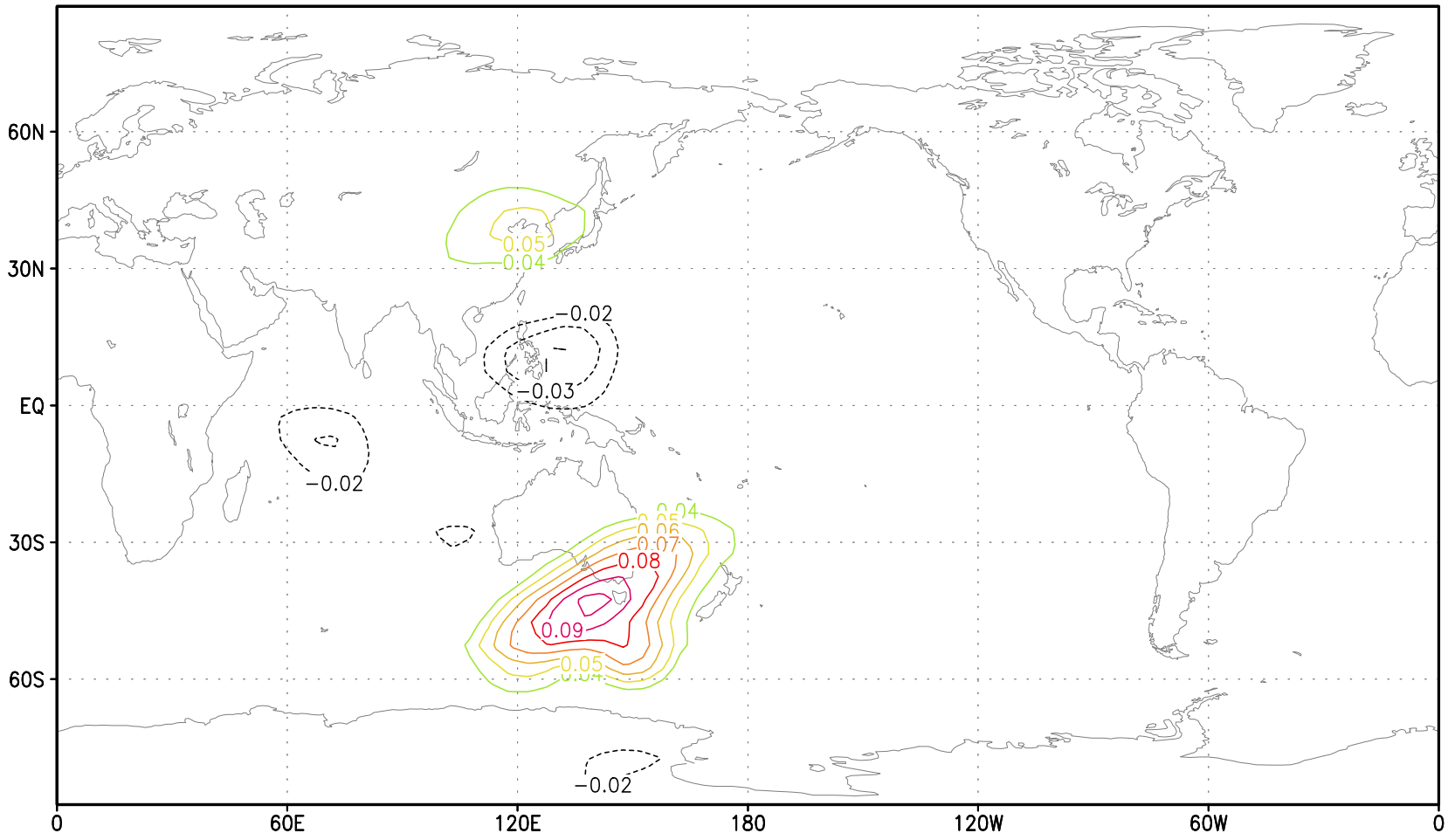
1st SV in zonal wind field, [6,24]h
60N
30N
EQ
30S
60S
0
60E
120E
180
120W
60W
0
0.05
0.04
−0.02
−0.03
−0.02
0.08
0.09
0.05
−0.02

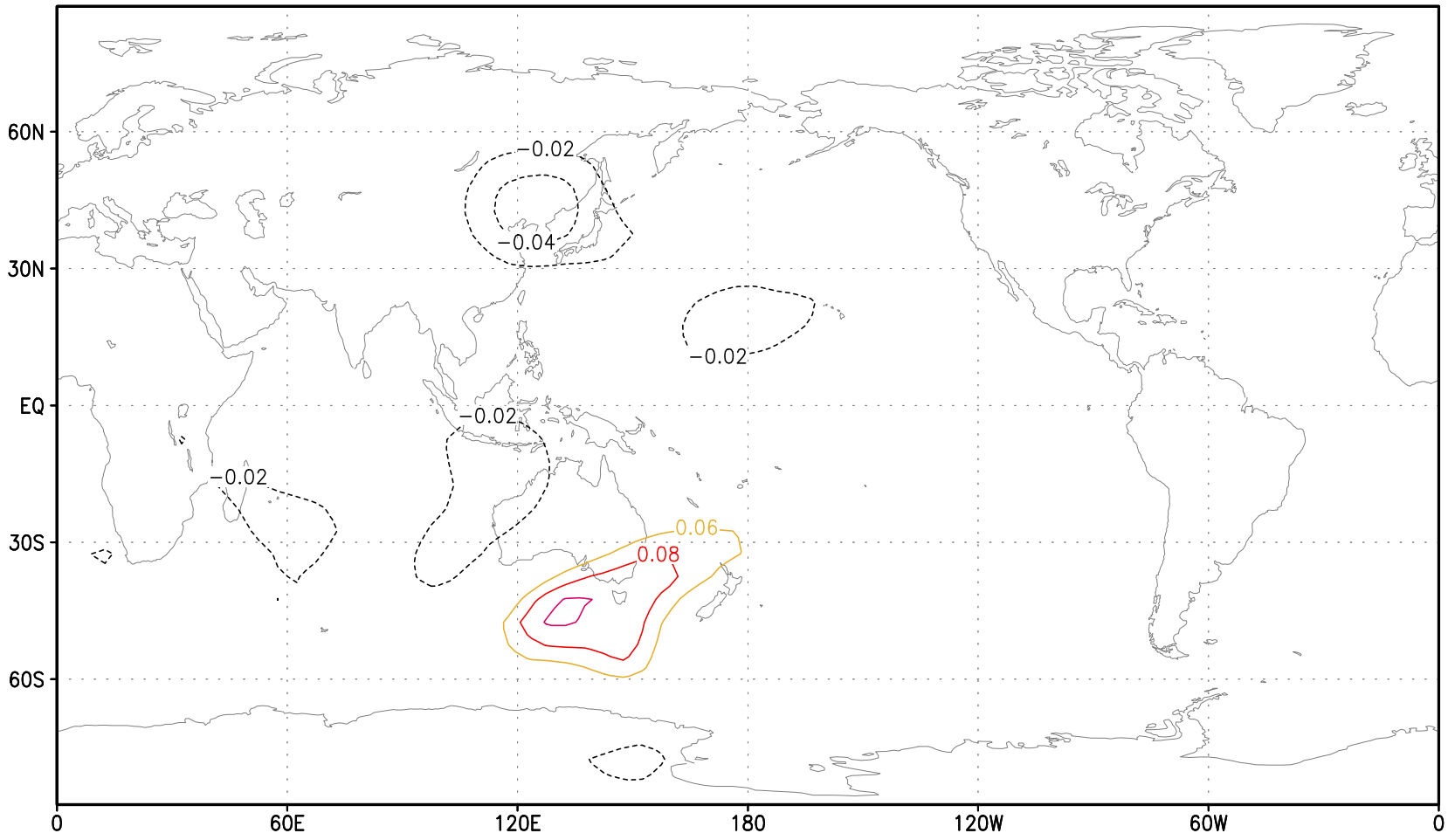
1st SV in zonal wind field, [2,24]h
60N
30N
EQ
30S
60S
0
60E
120E
180
120W
60W
0
−0.02
−0.04
−0.02
−0.02
−0.02
0.06
0.08

Target area definition using N leading singular Vectors

Consider the first N leading singular vectors $\nu_j, j = 1, 2, \ldots N$ at t_i with unit C-norm, $\|\nu_j\|_C = 1, j = 1, 2, \ldots N$.

Denote by $f_j^C(\lambda, \theta)$ the value of the C-norm of ν_j at grid point (λ, θ) (e.g. total energy norm at (λ, θ)).

Define the sensitivity function

$$F_N^C(\lambda, \theta) = \sum_{j=1}^{N} \left(\frac{\sigma_j}{\sigma_1} \right) f_j^C(\lambda, \theta); \qquad F_{MAX} = \max_{(\lambda,\theta)} F_N^C(\lambda, \theta) \tag{15}$$

The target area at t_i

$$\mathcal{D}_i = \{(\lambda, \theta) | F_N^C(\lambda, \theta) \geq 0.5 F_{MAX}\} \tag{16}$$

Observation locations at t_i are selected as first n_i locations (λ, θ) where $F_N^C(\lambda, \theta)$ has largest values.

Gradient Sensitivity Approach

Consider a perturbation $\delta \mathbf{x}_i$ of the model state at t_i and let

$$\delta \mathbf{x}_v = M(\mathbf{x}_i + \delta \mathbf{x}_i) - M(\mathbf{x}_i) \approx \mathbf{L}(t_i, t_v)\delta \mathbf{x}_i \tag{17}$$

be the induced perturbation at t_v.

To first order approximation,

$$\delta \mathcal{J}_v \approx \langle \mathbf{P}(\mathbf{x}_v - \mathbf{x}_v^{ref}), \delta \mathbf{x}_v \rangle_C \approx \langle \mathbf{L}^{*C}\mathbf{P}(\mathbf{x}_v - \mathbf{x}_v^{ref}), \delta \mathbf{x}_i \rangle_C \tag{18}$$

$$\nabla \mathcal{J}_v^C(\mathbf{x}_i) = \mathbf{L}^{*C}\mathbf{P}(\mathbf{x}_v - \mathbf{x}_v^{ref}) \tag{19}$$

Define the sensitivity function

$$F_v(\lambda, \theta) = \|\nabla \mathcal{J}_v^C(\lambda, \theta)\|_C \tag{20}$$

Observation locations at t_i: first n_i locations (λ, θ) where $F_v(\lambda, \theta)$ has

largest values.

Target area identification proceeds backward in time from t_I to t_1

An efficient evaluation of all $\nabla \mathcal{J}_v^C(\mathbf{x}_i), i = 1, 2, \ldots I$ is obtained through a single adjoint model integration.

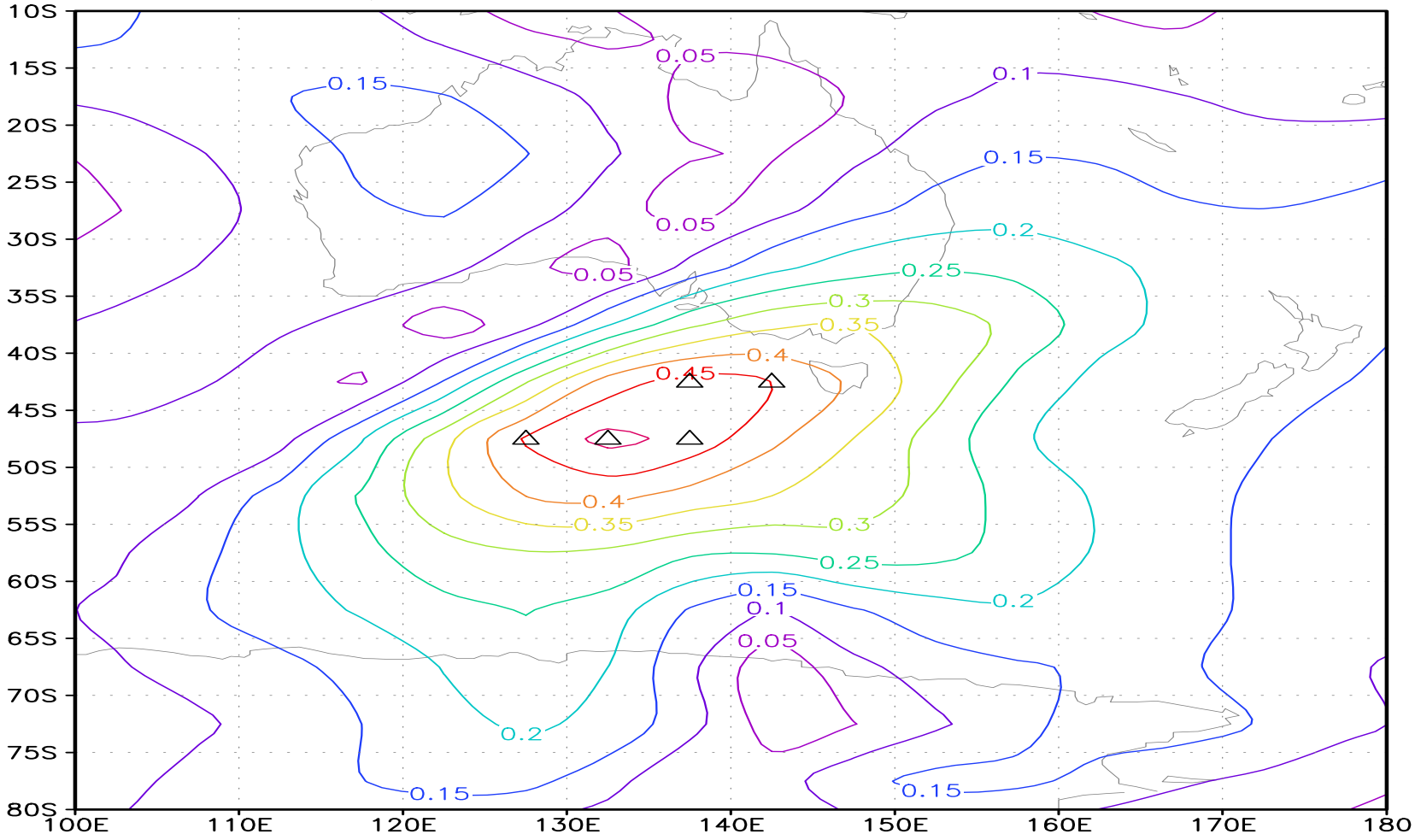
adaptive obs location at t=4h
10S
15S
20S
25S
30S
35S
40S
45S
50S
55S
60S
65S
70S
75S
80S
100E
110E
120E
130E
140E
150E
160E
170E
180
0.05
0.1
0.15
0.2
0.25
0.3
0.35
0.4
0.45

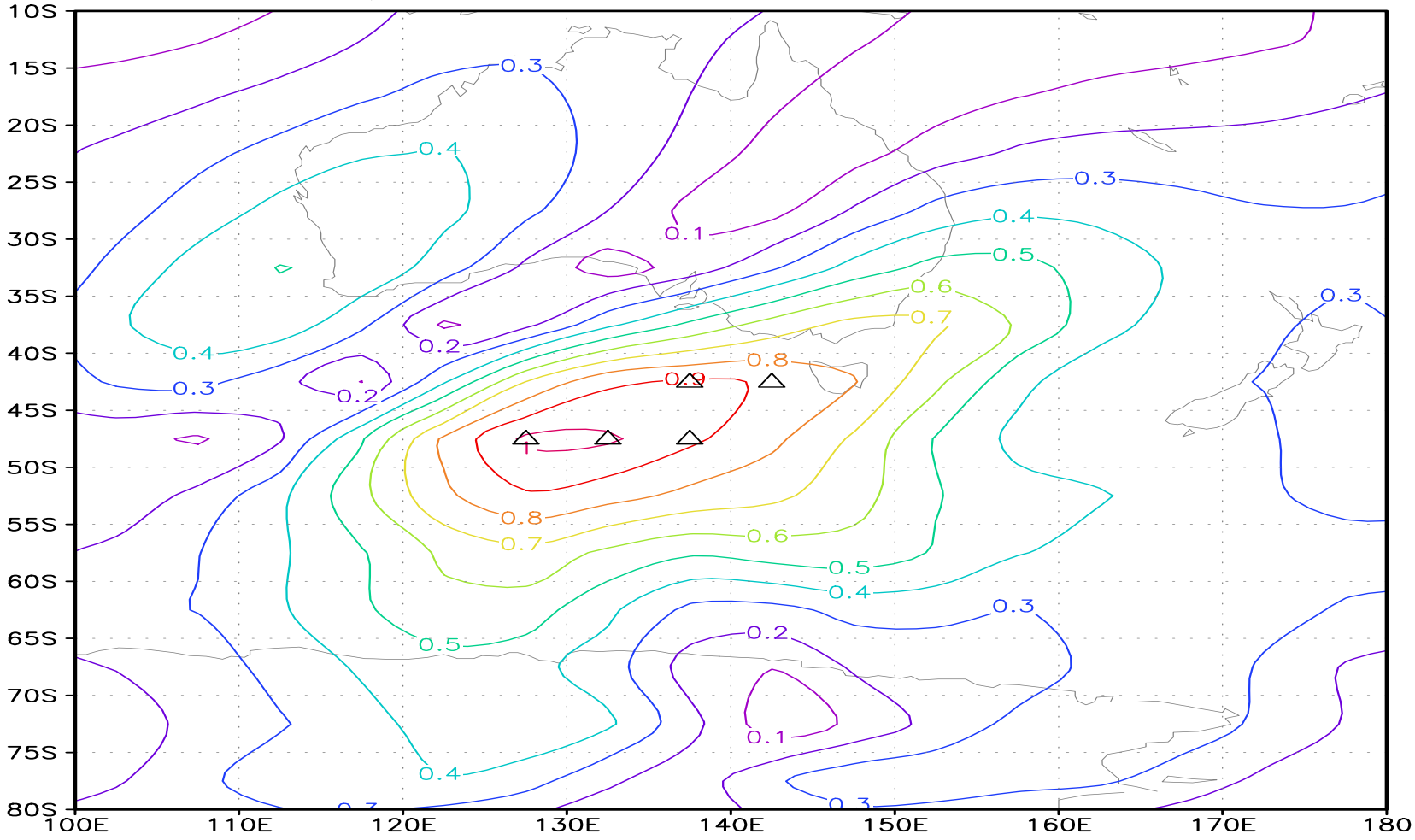
adaptive obs location at t=0h
10S
15S
20S
25S
30S
35S
40S
45S
50S
55S
60S
65S
70S
75S
80S
100E
110E
120E
130E
140E
150E
160E
170E
180
0.1
0.2
0.3
0.4
0.5
0.6
0.7
0.8
0.9

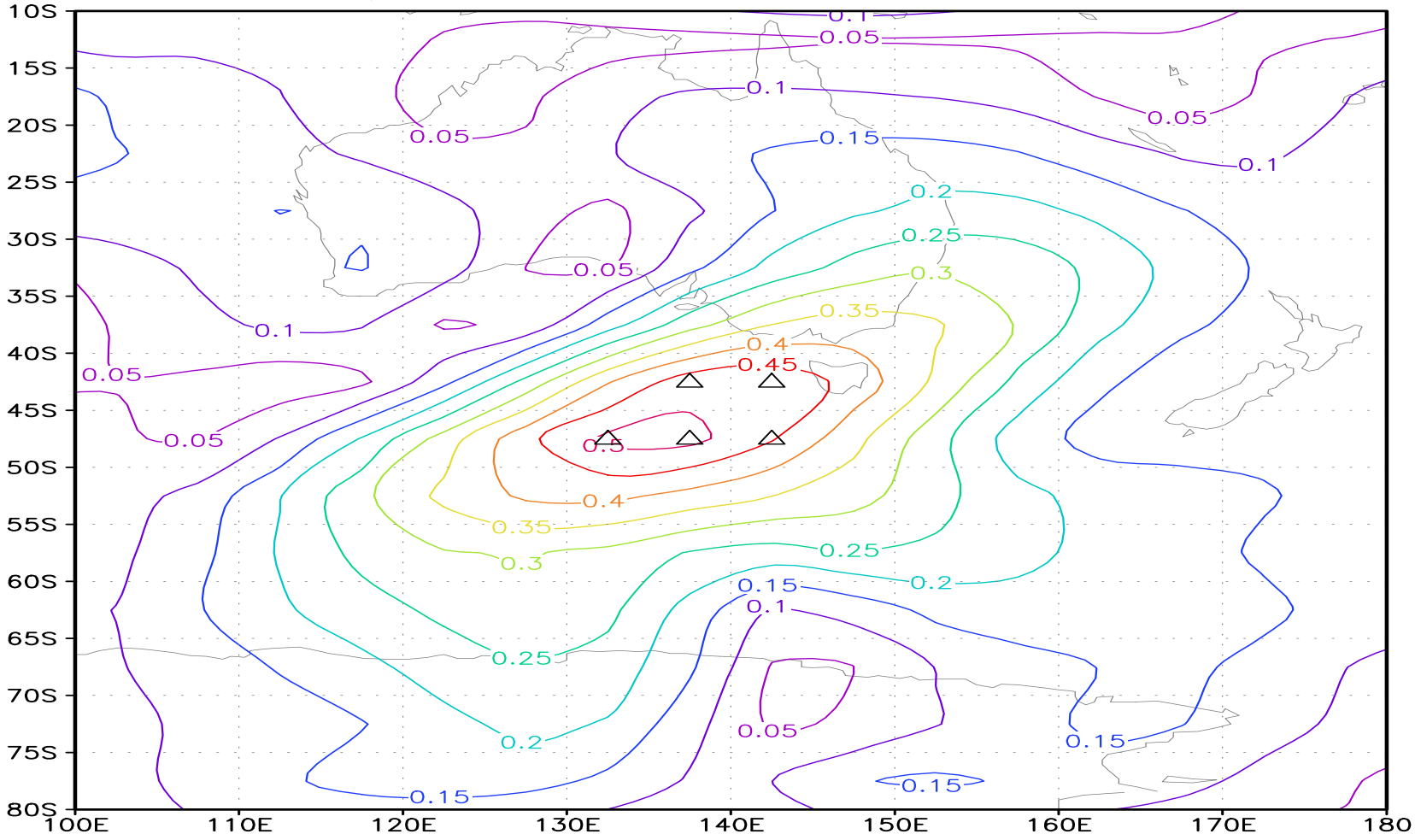
adaptive obs location at t=6h
10S
15S
20S
25S
30S
35S
40S
45S
50S
55S
60S
65S
70S
75S
80S
100E
110E
120E
130E
140E
150E
160E
170E
180
0.1
0.05
0.15
0.2
0.25
0.3
0.35
0.4
0.45
0.5

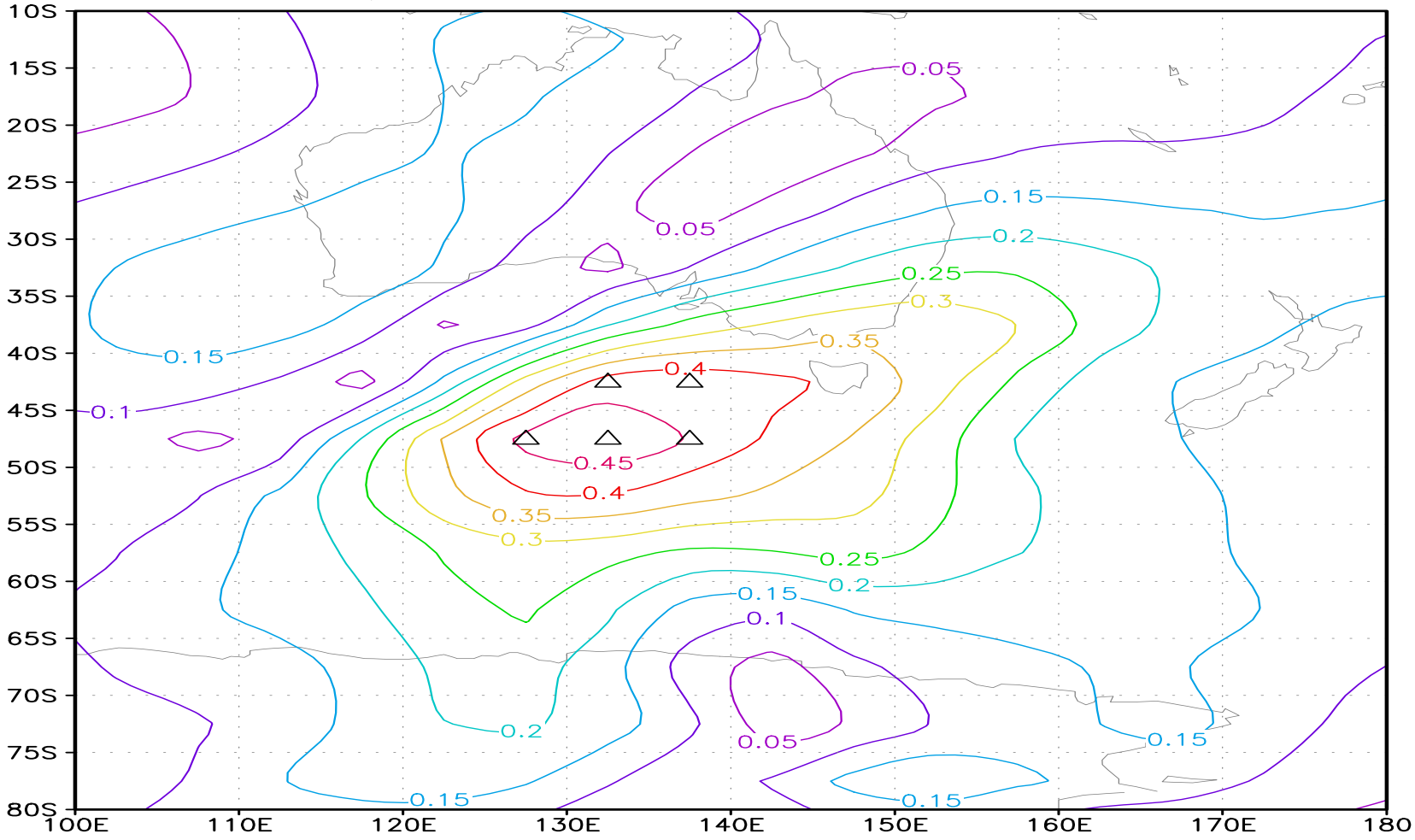
adaptive obs location at t=2h
10S
15S
20S
25S
30S
35S
40S
45S
50S
55S
60S
65S
70S
75S
80S
100E
110E
120E
130E
140E
150E
160E
170E
180
0.05
0.15
0.2
0.25
0.3
0.35
0.4
0.45
0.1

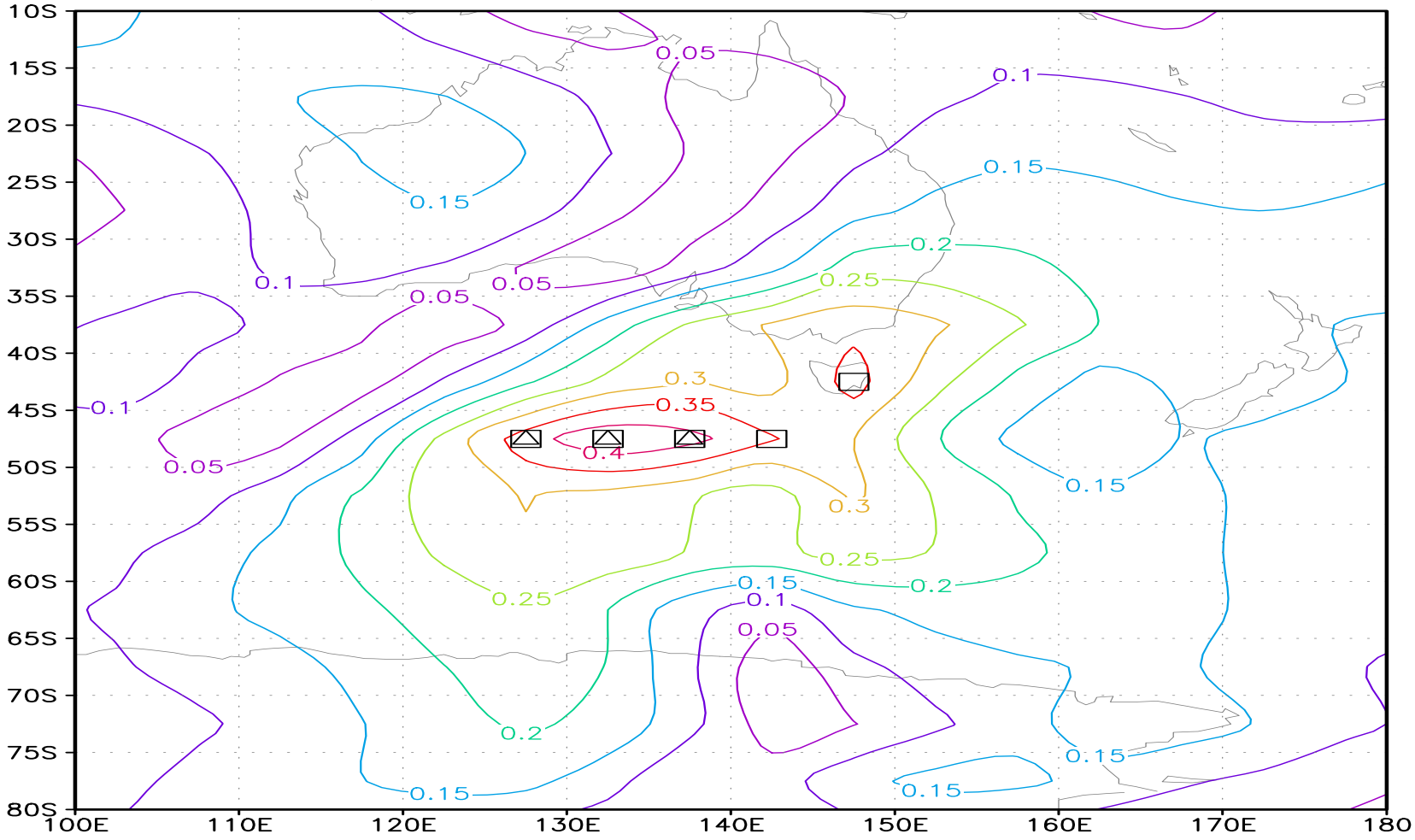
adaptive obs location at t=4h
10S
15S
20S
25S
30S
35S
40S
45S
50S
55S
60S
65S
70S
75S
80S
100E
110E
120E
130E
140E
150E
160E
170E
180
0.05
0.1
0.15
0.2
0.25
0.3
0.35
0.4

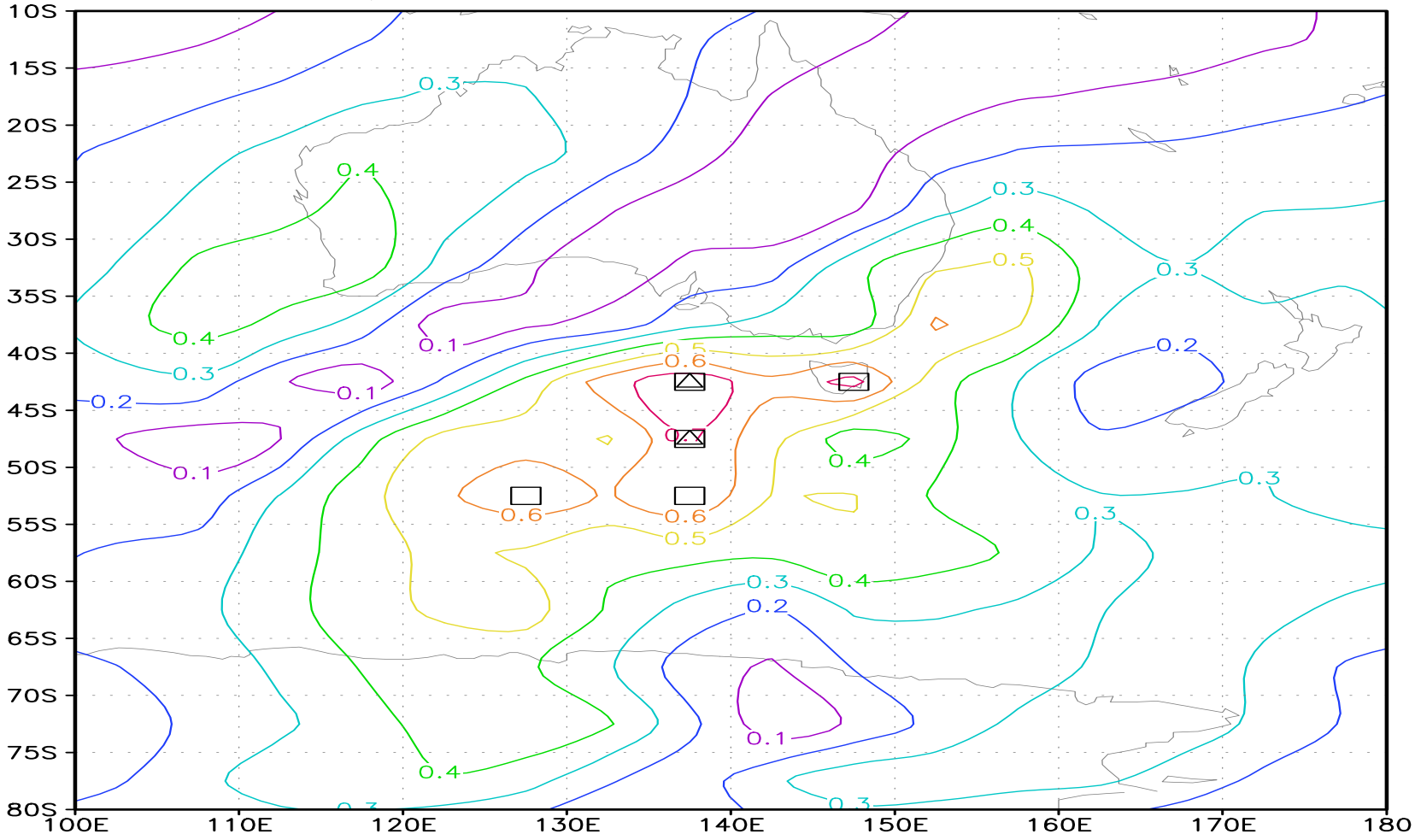
adaptive obs location at t=0h
10S
15S
20S
25S
30S
35S
40S
45S
50S
55S
60S
65S
70S
75S
80S
100E
110E
120E
130E
140E
150E
160E
170E
180
0.1
0.2
0.3
0.4
0.5
0.6

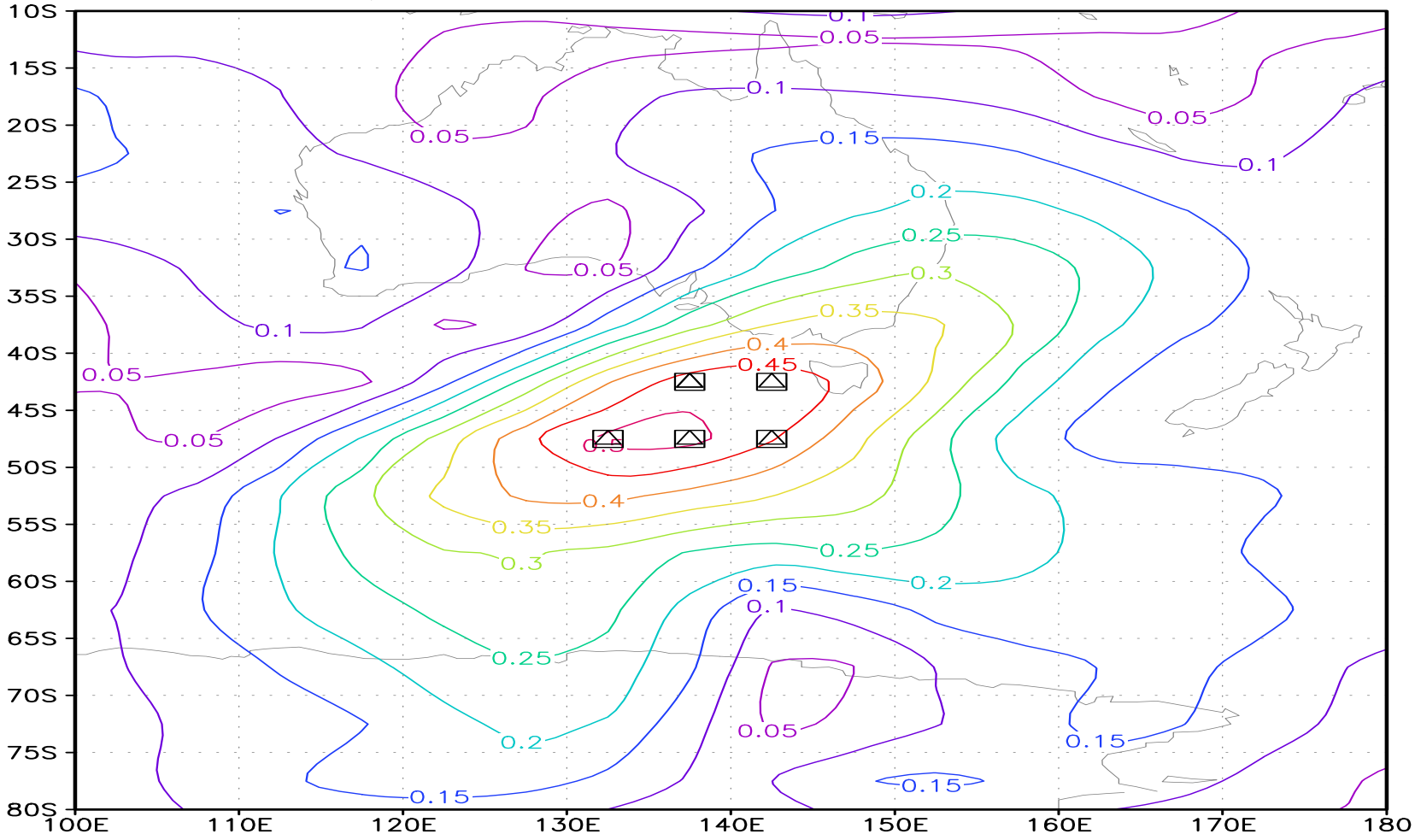
adaptive obs location at t=6h
10S
15S
20S
25S
30S
35S
40S
45S
50S
55S
60S
65S
70S
75S
80S
100E
110E
120E
130E
140E
150E
160E
170E
180
0.1
0.05
0.15
0.2
0.25
0.3
0.35
0.4
0.45

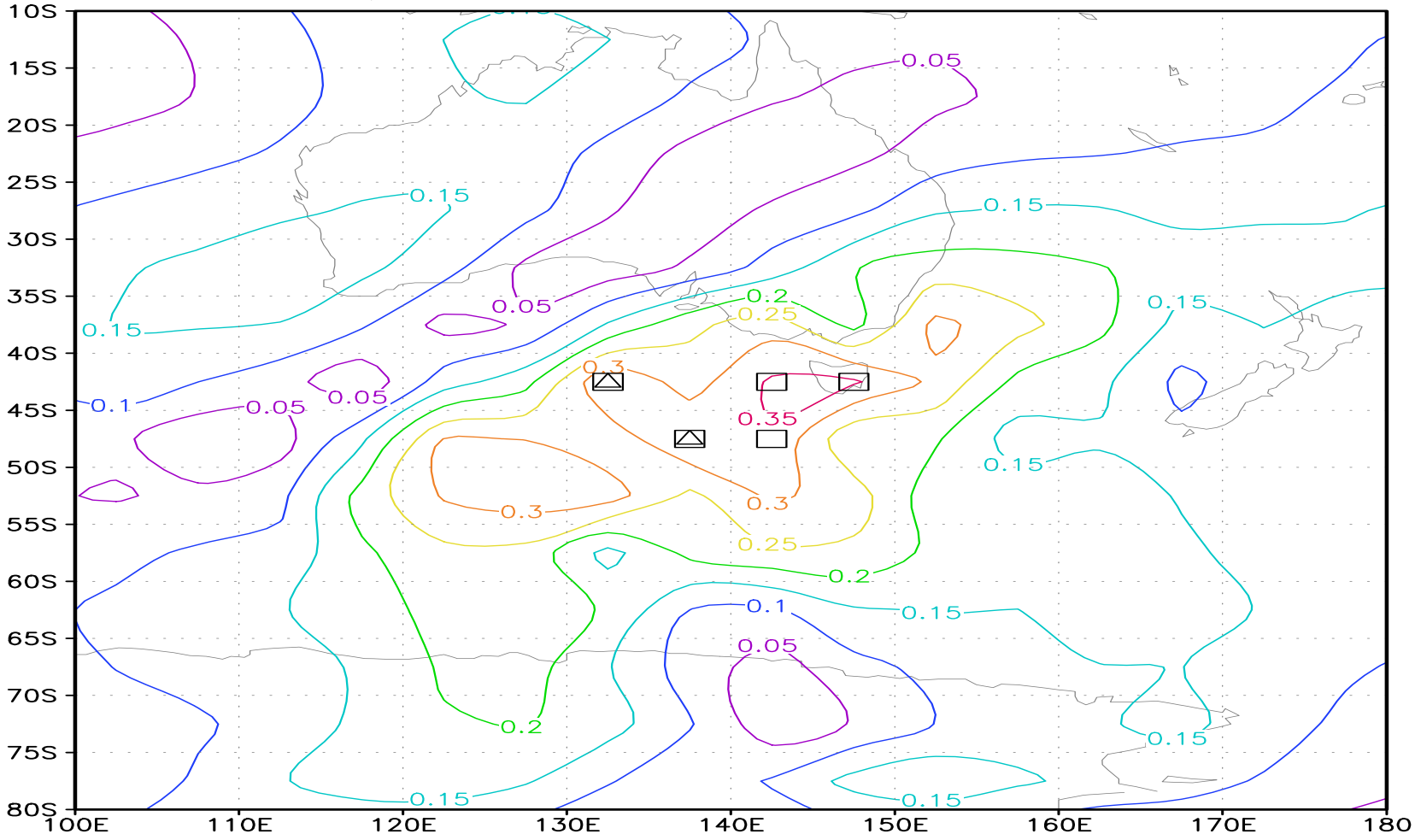
adaptive obs location at t=2h
10S
15S
20S
25S
30S
35S
40S
45S
50S
55S
60S
65S
70S
75S
80S
100E
110E
120E
130E
140E
150E
160E
170E
180
0.05
0.15
0.2
0.25
0.3
0.35
0.1

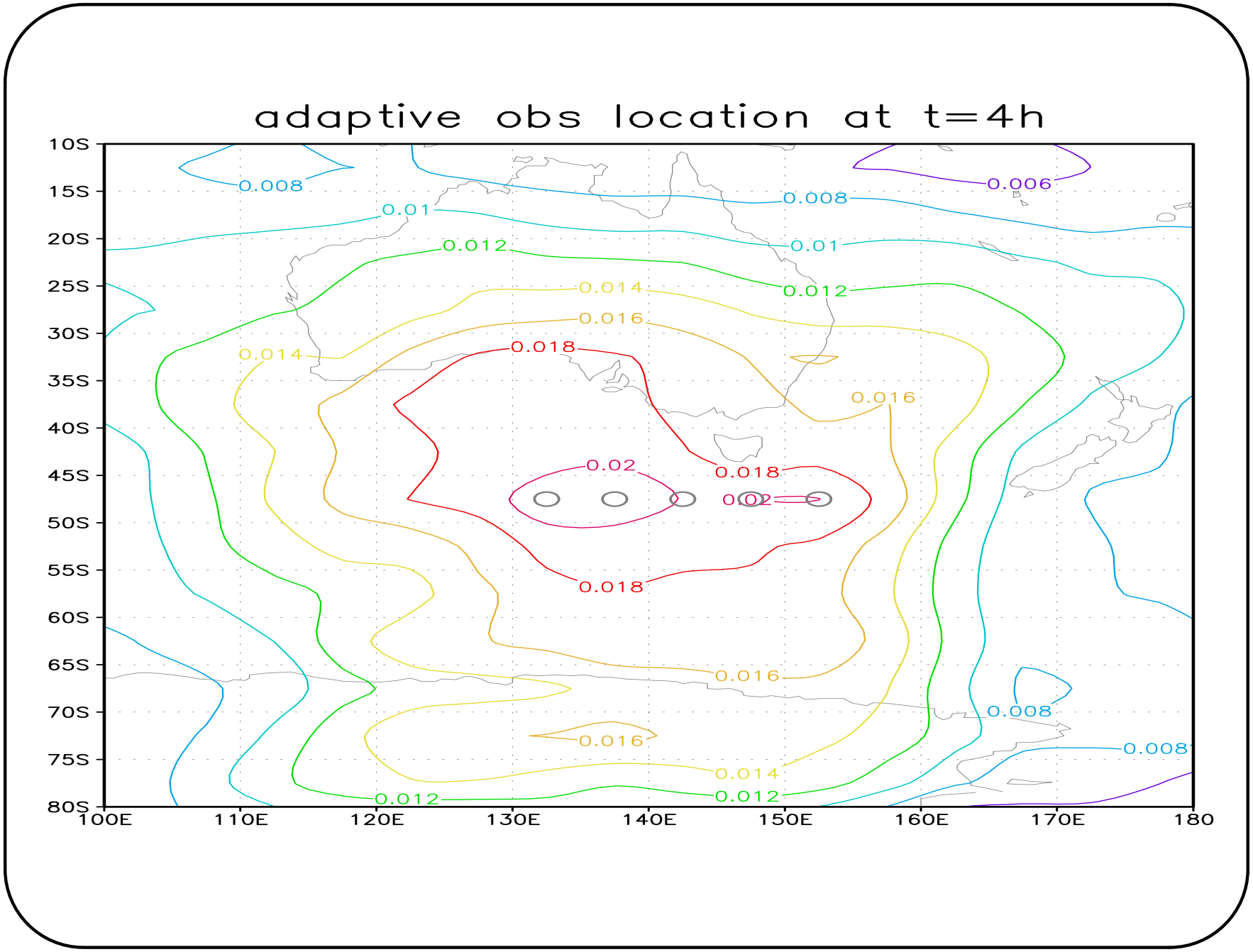
adaptive obs location at t=4h
10S
15S
20S
25S
30S
35S
40S
45S
50S
55S
60S
65S
70S
75S
80S
100E
110E
120E
130E
140E
150E
160E
170E
180
0.008
0.01
0.012
0.014
0.016
0.018
0.02
0.006

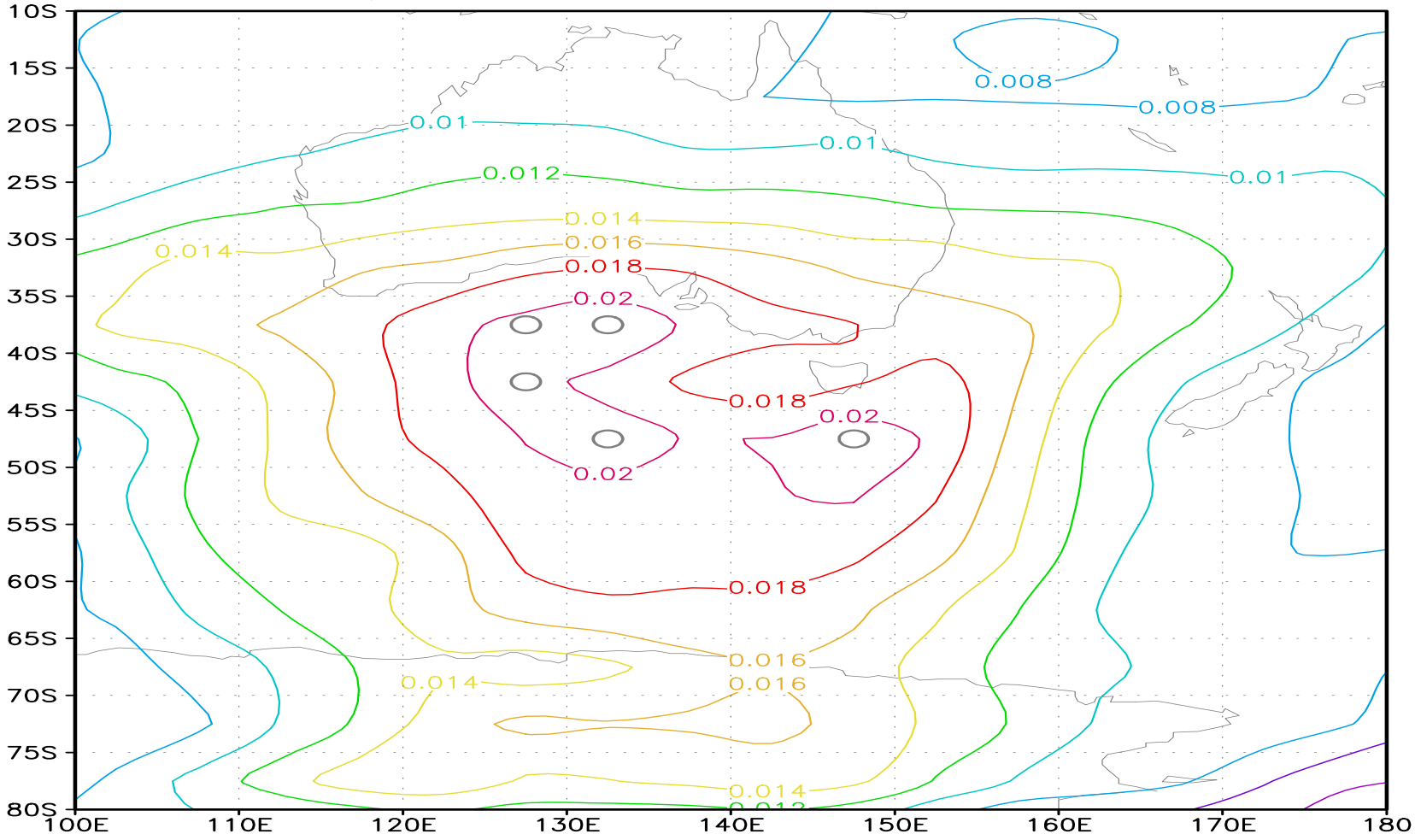
adaptive obs location at t=0h
10S
15S
20S
25S
30S
35S
40S
45S
50S
55S
60S
65S
70S
75S
80S
100E
110E
120E
130E
140E
150E
160E
170E
180
0.008
0.008
0.01
0.01
0.01
0.012
0.014
0.014
0.016
0.018
0.02
0.018
0.02
0.02
0.018
0.016
0.014
0.016
0.014

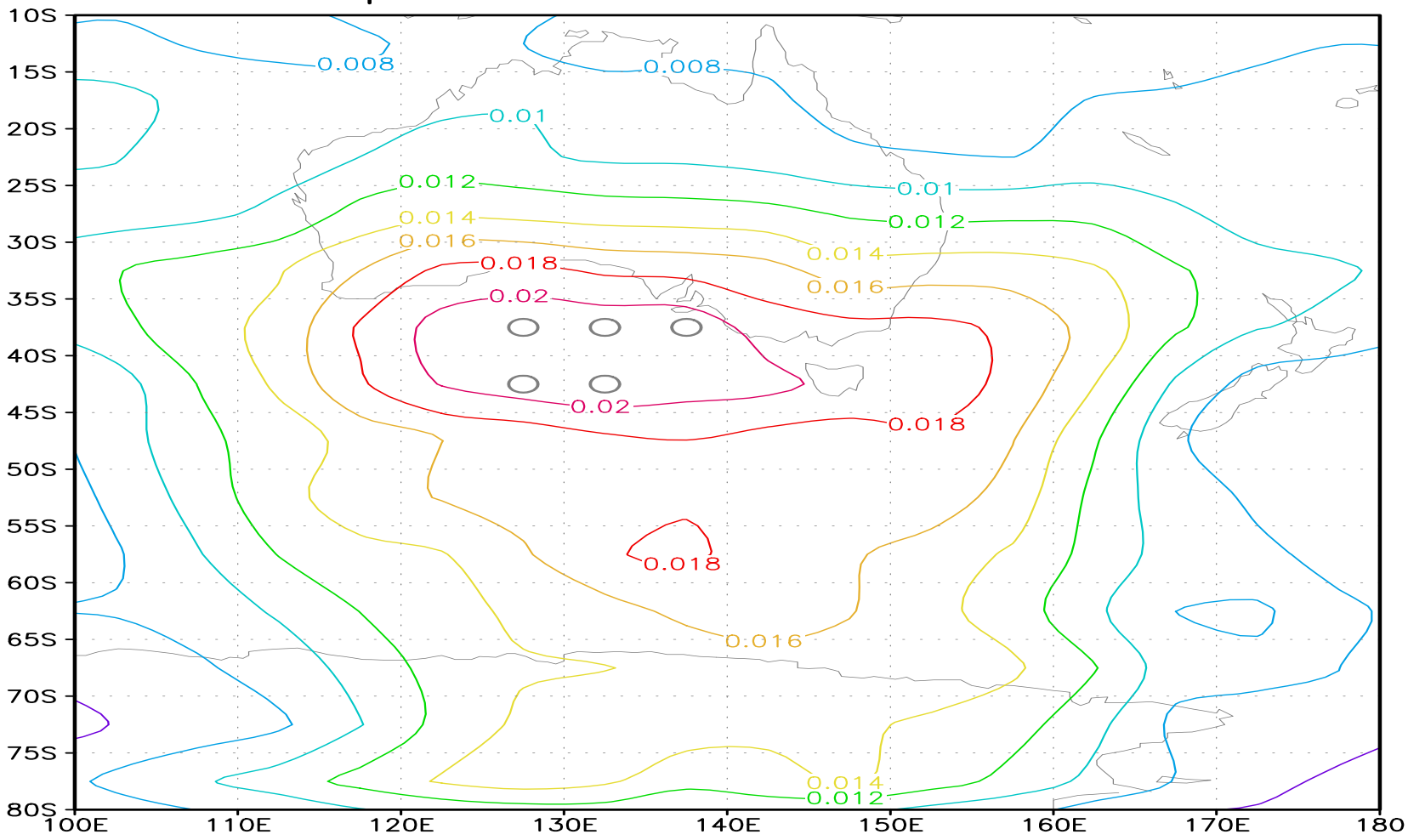
adaptive obs location at t=6h
10S
15S
20S
25S
30S
35S
40S
45S
50S
55S
60S
65S
70S
75S
80S
100E
110E
120E
130E
140E
150E
160E
170E
180
0.008
0.008
0.01
0.01
0.012
0.012
0.014
0.014
0.016
0.016
0.018
0.018
0.02
0.02
0.018
0.016
0.014
0.012

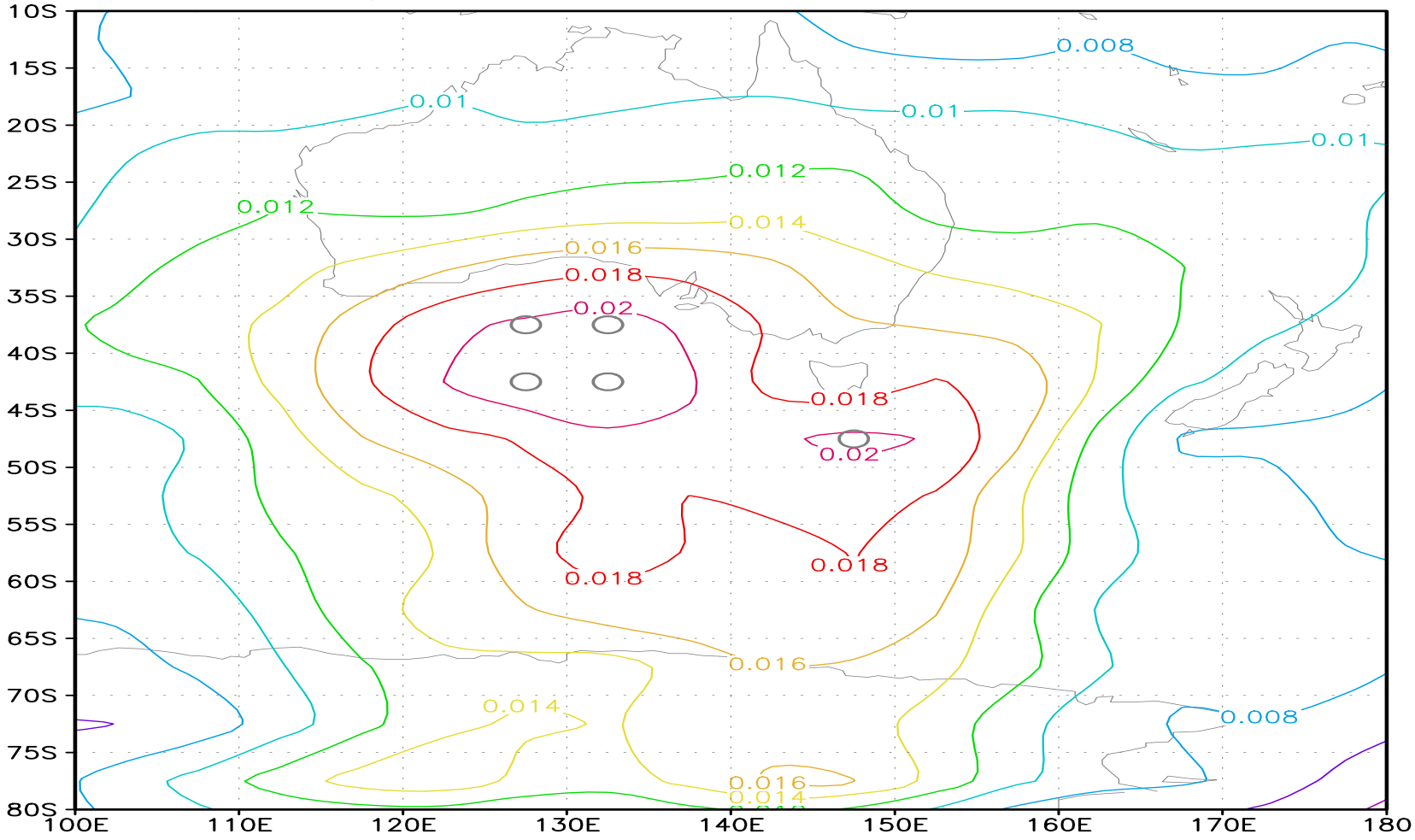
adaptive obs location at t=2h
10S
15S
20S
25S
30S
35S
40S
45S
50S
55S
60S
65S
70S
75S
80S
100E
110E
120E
130E
140E
150E
160E
170E
180
0.008
0.01
0.01
0.01
0.012
0.012
0.014
0.016
0.018
0.02
0.018
0.02
0.018
0.018
0.016
0.014
0.008
0.016
0.014

Practical Issues

Baker and Daley (QJRMS 2000) noticed that the 'a priori' evaluation of the sensitivity vector is completely ignorant of any existing observations.

Suppose that two sensitivity regions have been identified: one of them of much greater amplitude than the other but with a satellite pass over it, while the smaller amplitude target is in a relatively data void region.

Q: which is the higher-priority target, if operational considerations permit only one to be sampled?

Q: what is the most efficient way to sample adequately a sensitivity gradient field in the presence of existing observations?

4D-Var takes into consideration *all* available observations in the assimilation window.

Optimal adaptive observations at t_i have been determined assuming that these are *the only* available observations.

> **Q:** If individually each of $\mathcal{O}_i^a$ at t_i and $\mathcal{O}_{i+1}^a$ at t_{i+1} is an optimal adaptive observations set, is $\{\mathcal{O}_i^a, \mathcal{O}_{i+1}^a\}$ still optimal?

Interaction between observations must be considered.

Interaction between adaptive observations

Our new sensitivity approach takes into consideration the interaction between adaptive observations at distinct instants in time and the interaction with routine observations (a priori known locations).

A periodic update of the adjoint sensitivity field at t_i is performed which takes into consideration all observations already located at t_{i+1}.

Denote by

$$\mathcal{O}_{i+1} = \mathcal{O}^f \cup \mathcal{O}_I^a \cup \ldots \cup \mathcal{O}_{i+1}^a \tag{21}$$

the set of all observations already located at time t_{i+1} and consider $\mathcal{J}_{\mathcal{O}_{i+1}}(\mathbf{x}_i)$ the cost functional $\mathcal{J}$ restricted to the observational set $\mathcal{O}_{i+1}$ as a function $\mathbf{x}_i$.

We introduce a new sensitivity field associated to the observations set $\mathcal{O}_{i+1}$

$$F_i(\lambda, \theta) = \|\nabla \mathcal{J}_{\mathcal{O}_{i+1}}(\lambda, \theta)\| \tag{22}$$

and update the sensitivity field F_v at t_i according to

$$F_v(\lambda, \theta) = F_v(\lambda, \theta) \left(1 + \alpha \frac{F_i(\lambda, \theta)}{F_v(\lambda, \theta)}\right)^{-1} \tag{23}$$

The updated sensitivity field is inversely proportional to the relative value of the sensitivity field provided by the set of observations that have been already located.

The additional computational cost to evaluate the sensitivity F_i is given by the computational cost of a backward integration in the assimilation window $[t_0\ T]$.

New observations at t_i are located in regions where the sensitivity of $\mathcal{J}_v$ to the model state is large *and* little additional information may be obtained from previously located observations.

The interaction between observations may be controlled by the weight coefficient α which may reflect our confidence in the previously selected observations (e.g. observational errors).

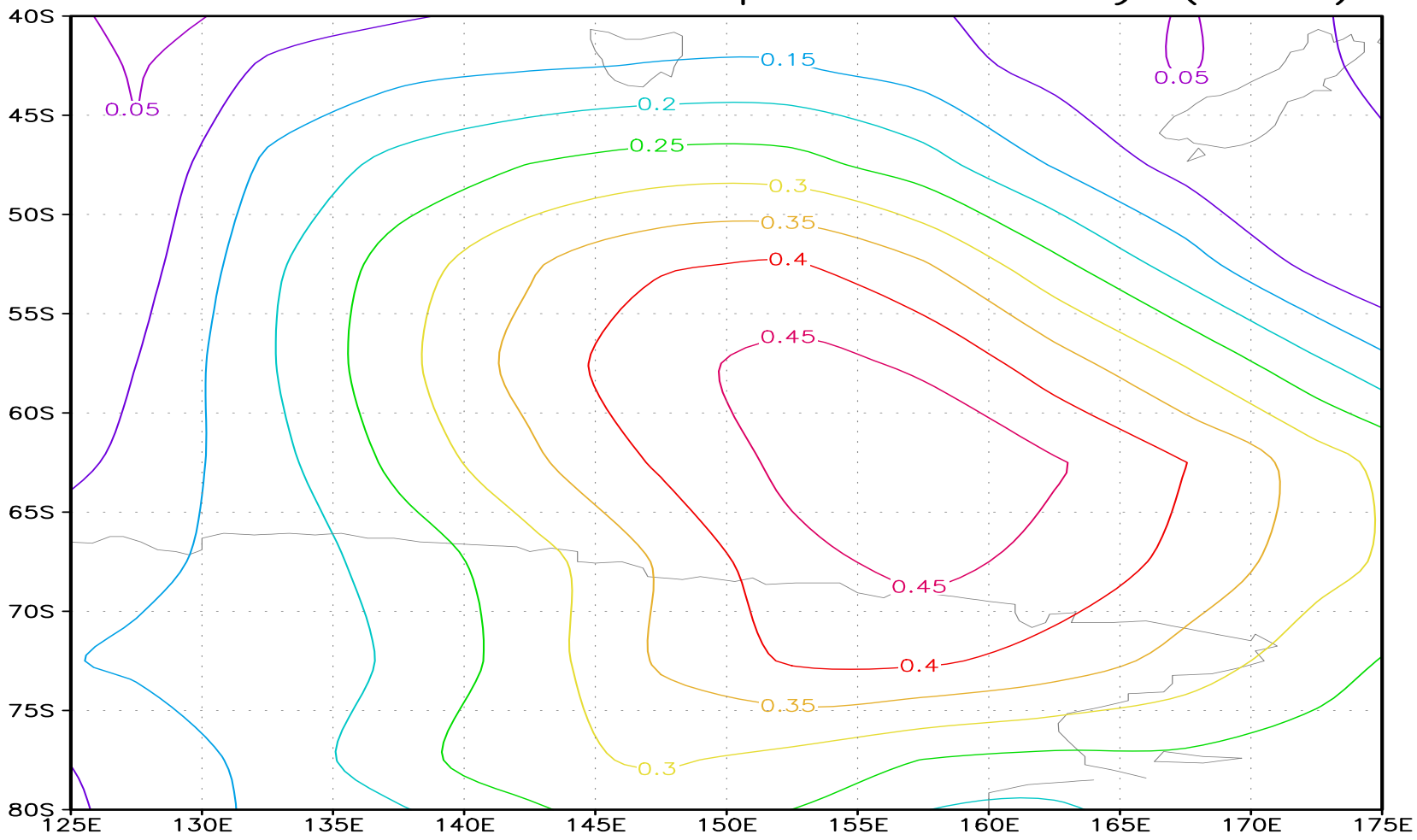
error at 24h with adaptive obs only (TESV)
40S
45S
50S
55S
60S
65S
70S
75S
80S
125E
130E
135E
140E
145E
150E
155E
160E
165E
170E
175E
0.05
0.15
0.2
0.25
0.3
0.35
0.4
0.45

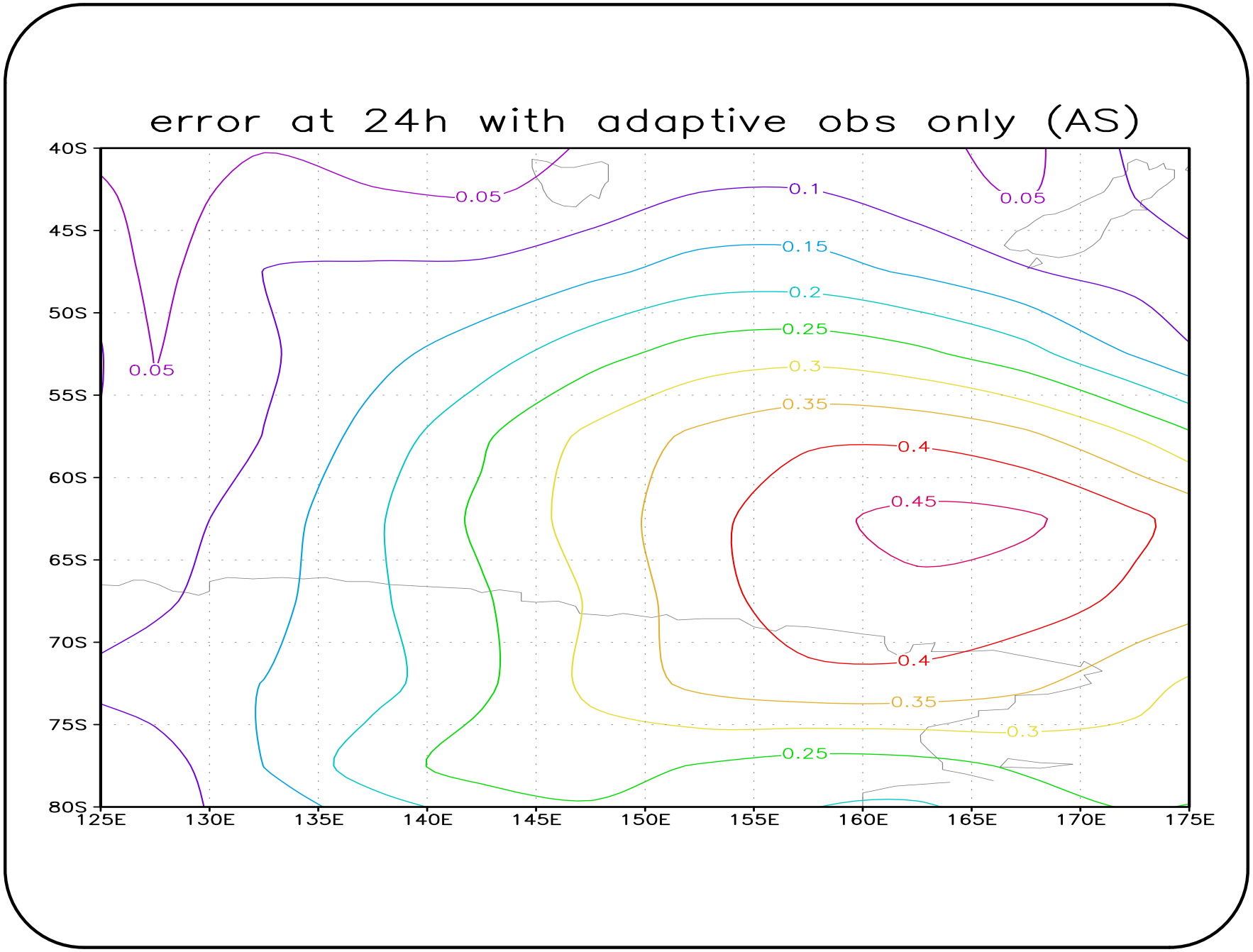
error at 24h with adaptive obs only (AS)
40S
45S
50S
55S
60S
65S
70S
75S
80S
125E
130E
135E
140E
145E
150E
155E
160E
165E
170E
175E
0.05
0.1
0.15
0.2
0.25
0.3
0.35
0.4
0.45

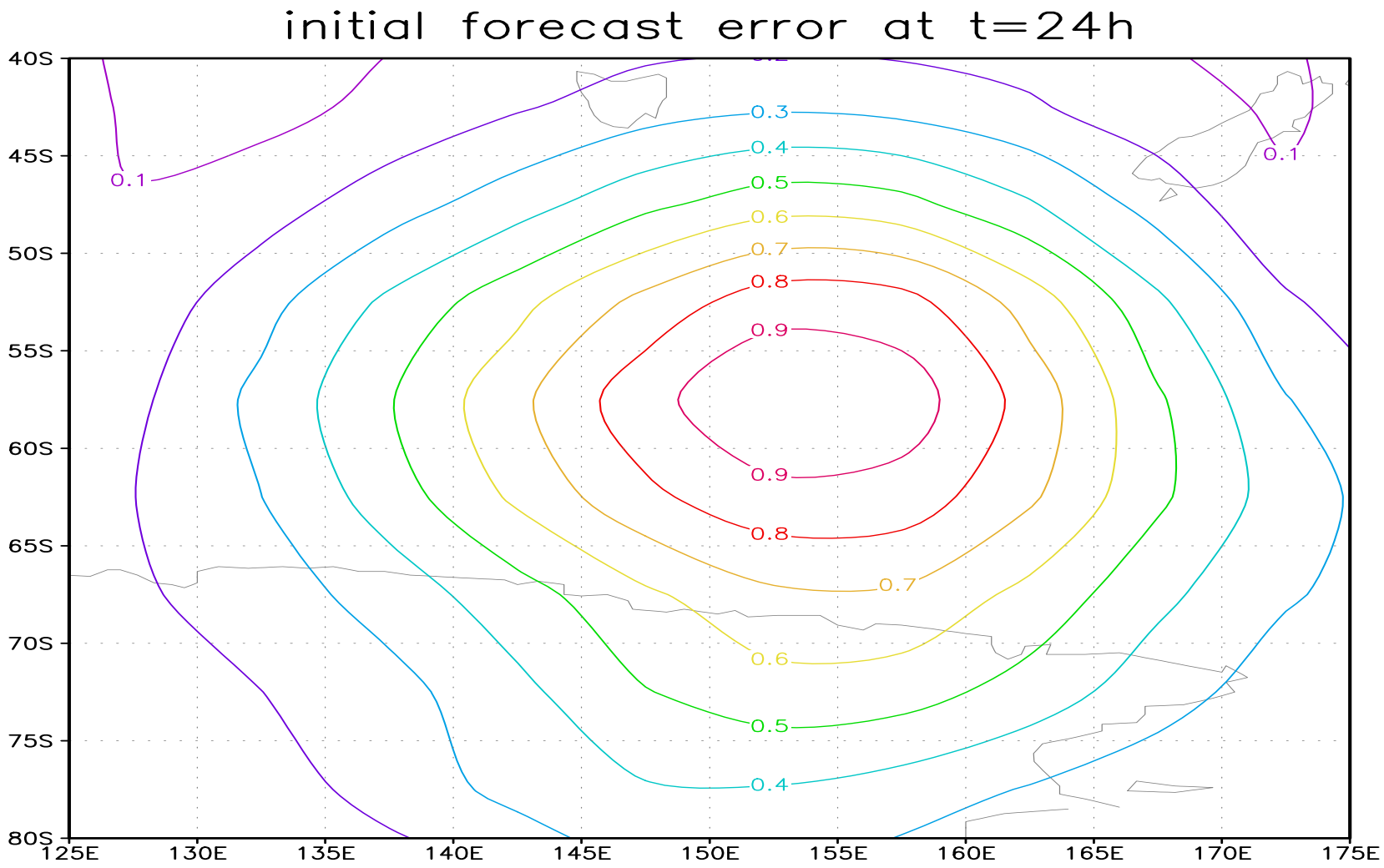
initial forecast error at t=24h
40S
45S
50S
55S
60S
65S
70S
75S
80S
125E
130E
135E
140E
145E
150E
155E
160E
165E
170E
175E
0.1
0.3
0.4
0.5
0.6
0.7
0.8
0.9
0.9
0.8
0.7
0.6
0.5
0.4
0.1

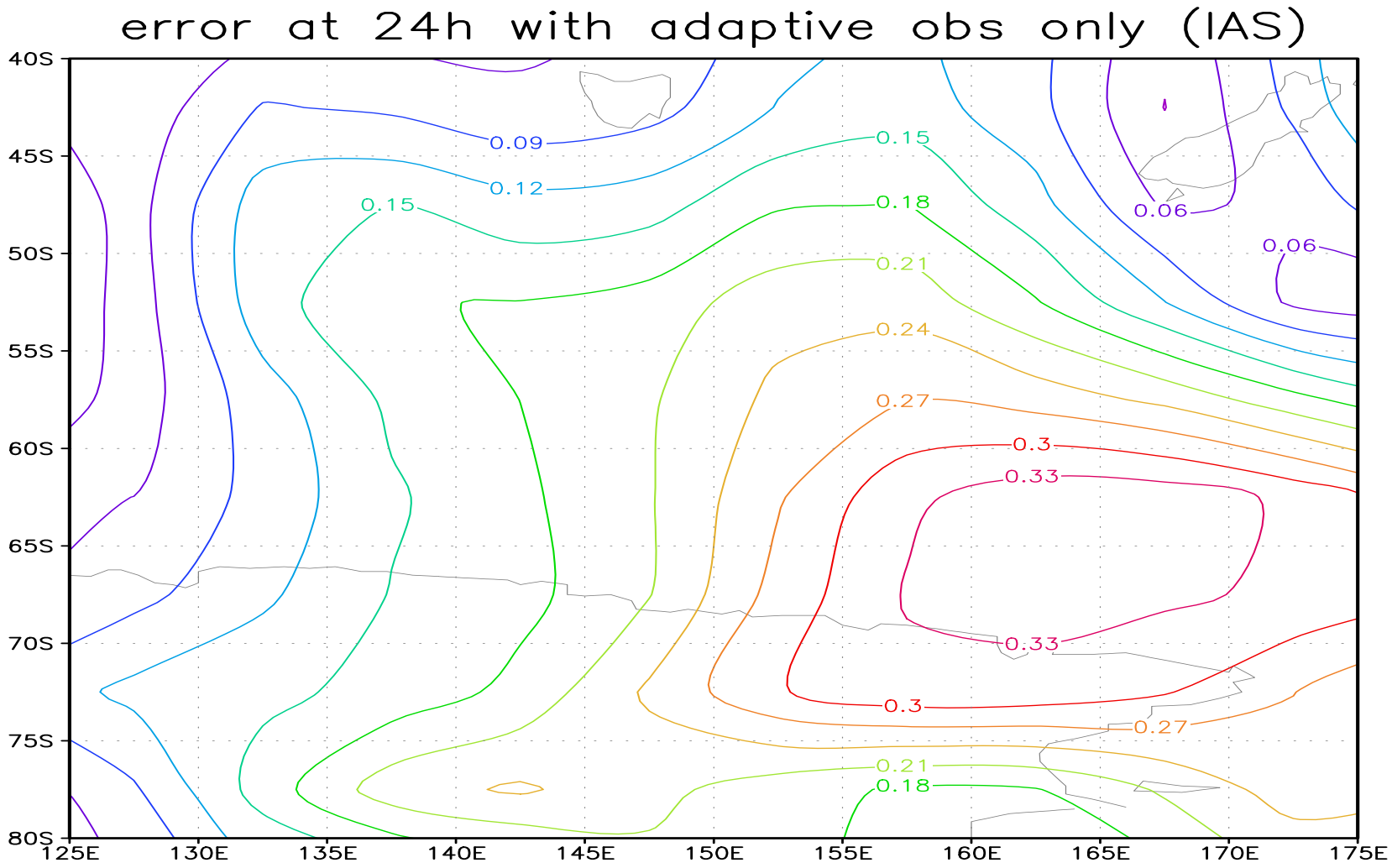
error at 24h with adaptive obs only (IAS)
40S
45S
50S
55S
60S
65S
70S
75S
80S
125E
130E
135E
140E
145E
150E
155E
160E
165E
170E
175E
0.09
0.12
0.15
0.15
0.18
0.21
0.24
0.27
0.3
0.33
0.33
0.3
0.27
0.21
0.18
0.06
0.06

Numerical experiments settings

4D-Var data assimilation is performed in the assimilation window $[0-6]$h in the twin experiments framework.

A background field is prescribed using a 5% random perturbation in the reference velocities field.

Observations at fixed location are prescribed at t=6h only, on a $20^\circ \times 20^\circ$ grid subdomain.

We assume that each hour in the interval $[0-6]$h five adaptive observations may be selected and their optimal location must be determined by an appropriate targeting procedure.

A forecast starting from the background estimate shows large errors at the verification time $t_v = 24$h over the spatial domain
$\mathcal{D}_v = [125^\circ\text{E}\ 175^\circ\text{E}] \times [80^\circ\text{S}\ 40^\circ\text{S}]$ which is selected as the verification domain.

Targeting strategies using the leading singular vectors (first 10), gradient sensitivity, and gradient sensitivity with interaction between adaptive observations are compared in two experiments:

- In the first experiment a comparative analysis of the forecast error at $t_v = 24$h over $\mathcal{D}_v$ is considered when *only the adaptive observations* are included in the data assimilation process.
- In the second experiment both the fixed and adaptive observations are included in the data assimilation and the forecast error at t_v over $\mathcal{D}_v$ is compared against the forecast error corresponding to a data assimilation using only observations from fixed locations.

The total energy norm is used to define the inner product $\langle \cdot, \cdot \rangle_C$ (diagonal C), and the forecast error at t_v is quantified in the total energy norm.

For each method the time evolution of the sensitivity field and the corresponding adaptive observations locations is displayed at t=6h, 4h, 2h, 0h as follows:

$'\triangle'$ - adaptive observations selected by the gradient sensitivity method with no interactions (adj).

$'\square'$ - adaptive observations selected by the gradient sensitivity method with interactions (inter-adj).

$'\circ'$ - adaptive observations selected by the singular vectors method (svd)

For each method, during the data assimilation process to minimize the cost functional $\mathcal{J}$ (over the entire domain) we also monitor the evolution of the forecast error reduction $\mathcal{J}_v(\mathbf{x}_0^\star)/\mathcal{J}_v(\mathbf{x}_0)$ at t_v over $\mathcal{D}_v$.

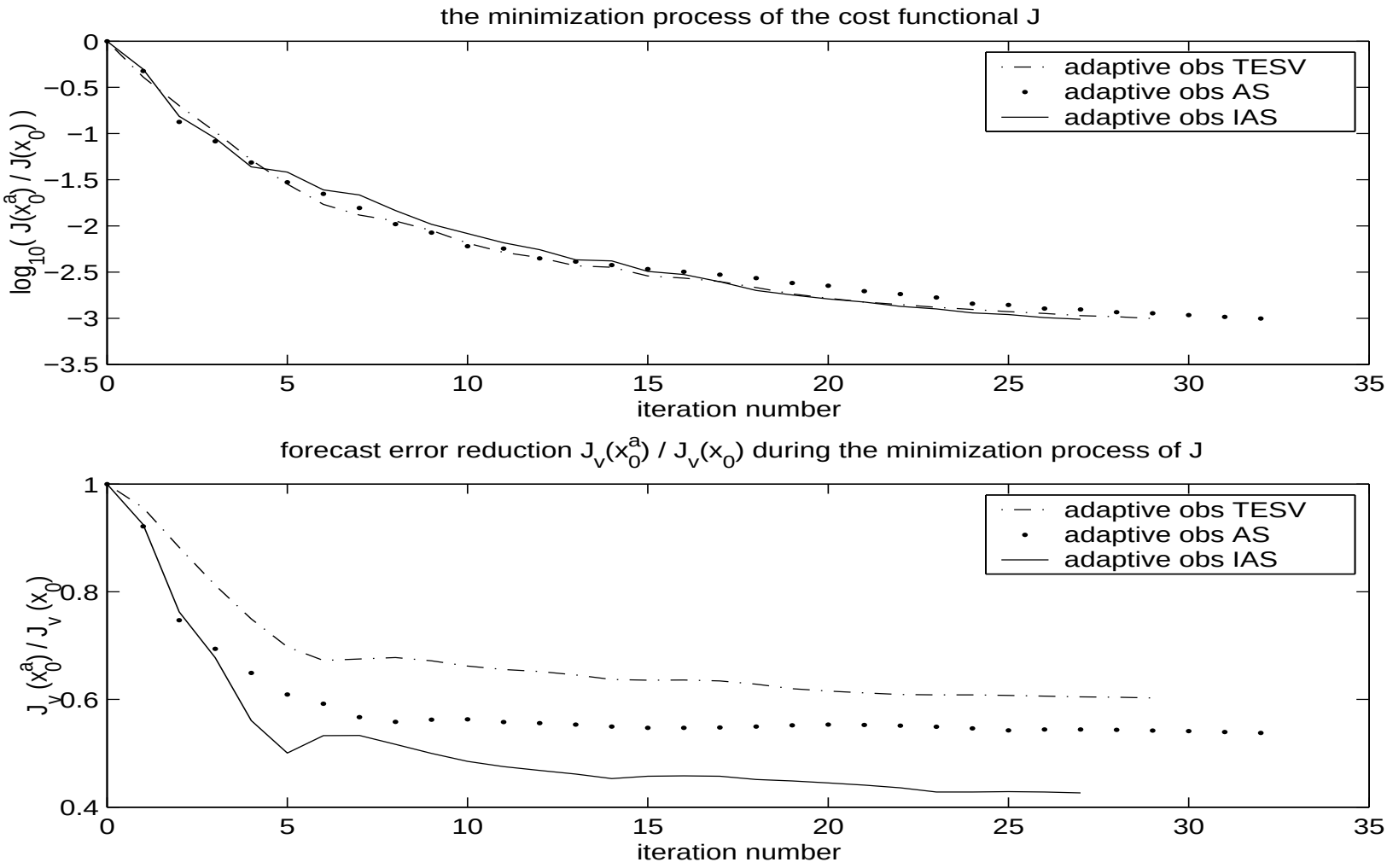
the minimization process of the cost functional J
adaptive obs TESV
adaptive obs AS
adaptive obs IAS
iteration number
forecast error reduction J_v(x_0^a) / J_v(x_0) during the minimization process of J
adaptive obs TESV
adaptive obs AS
adaptive obs IAS
iteration number

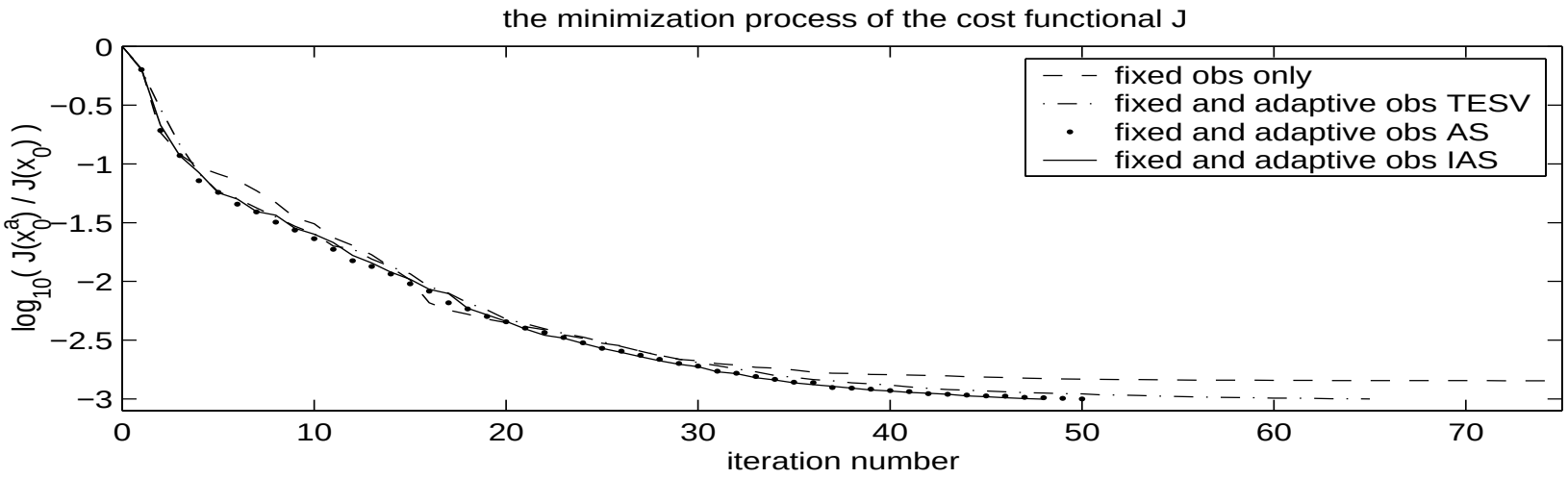
the minimization process of the cost functional J
fixed obs only
fixed and adaptive obs TESV
fixed and adaptive obs AS
fixed and adaptive obs IAS
log10(J(x0a) / J(x0))
iteration number

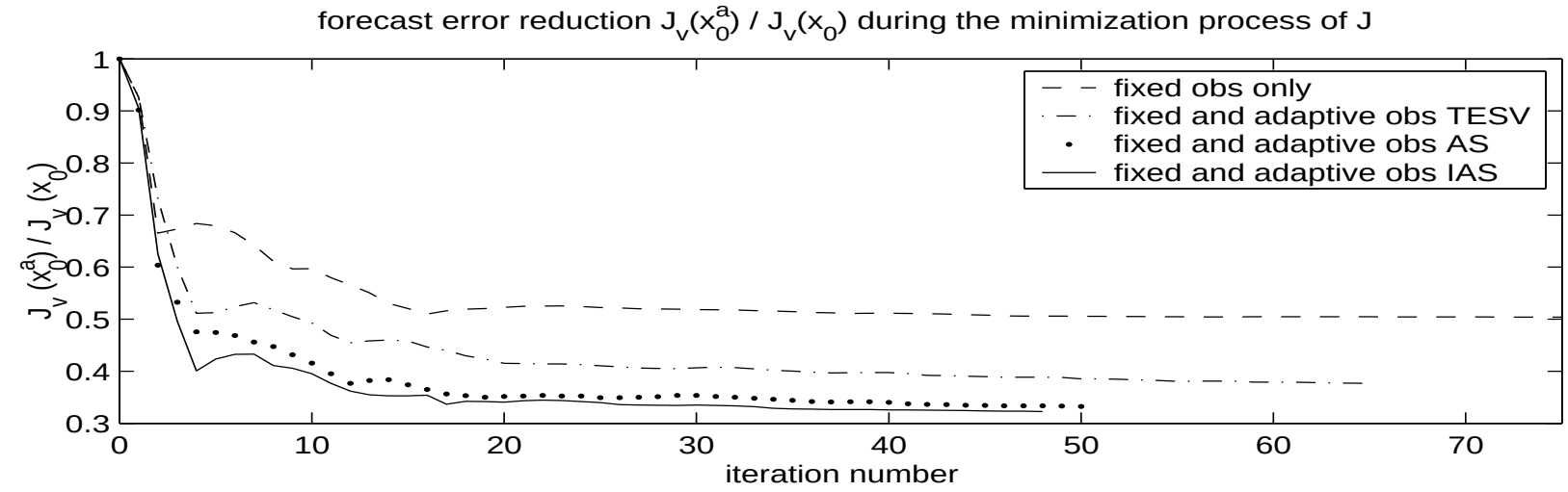
forecast error reduction Jv(x0a) / Jv(x0) during the minimization process of J
fixed obs only
fixed and adaptive obs TESV
fixed and adaptive obs AS
fixed and adaptive obs IAS
Jv (x0a) / Jv (x0)
iteration number

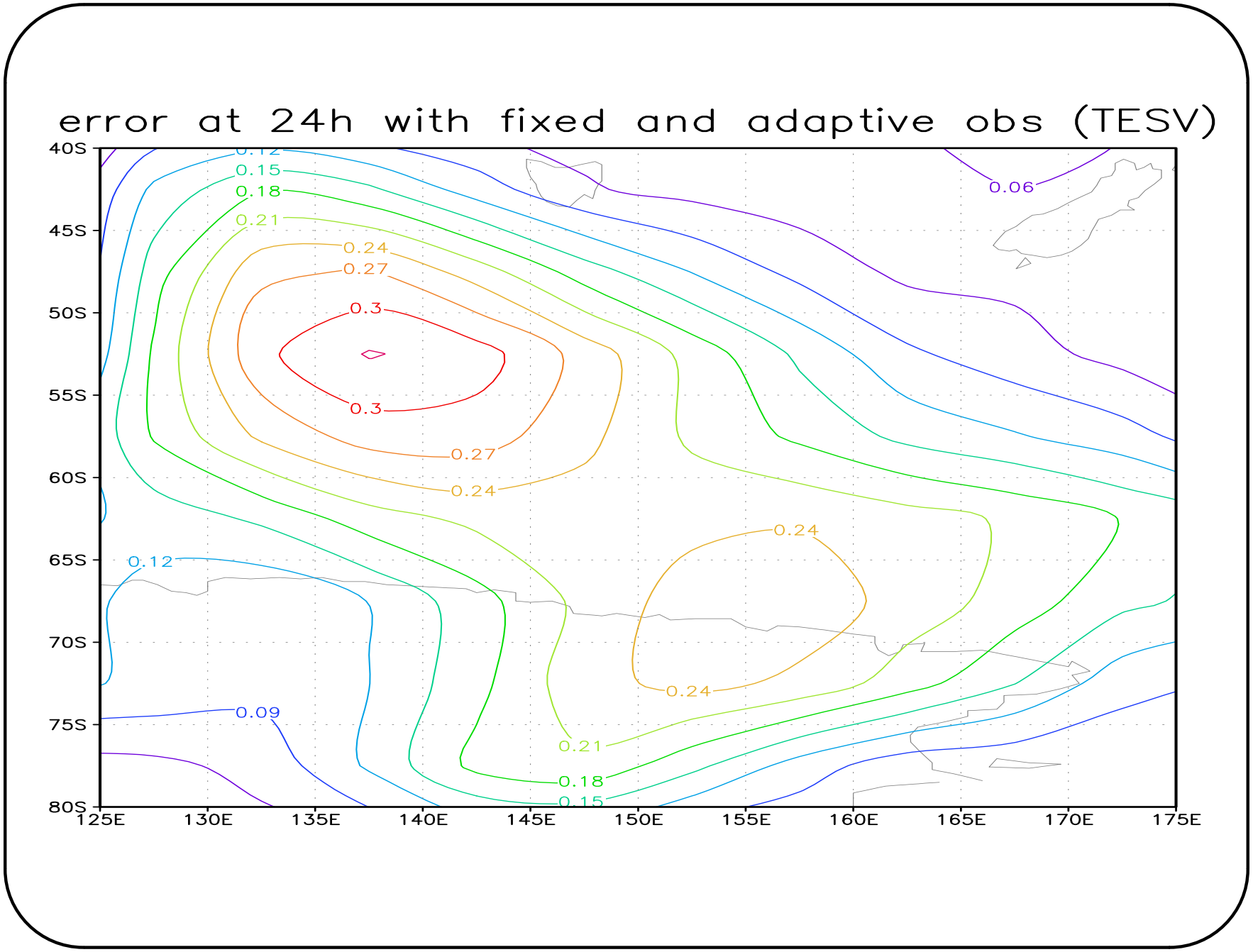
error at 24h with fixed and adaptive obs (TESV)
40S
45S
50S
55S
60S
65S
70S
75S
80S
125E
130E
135E
140E
145E
150E
155E
160E
165E
170E
175E
0.06
0.15
0.18
0.21
0.24
0.27
0.3
0.3
0.27
0.24
0.12
0.24
0.24
0.09
0.21
0.18
0.15

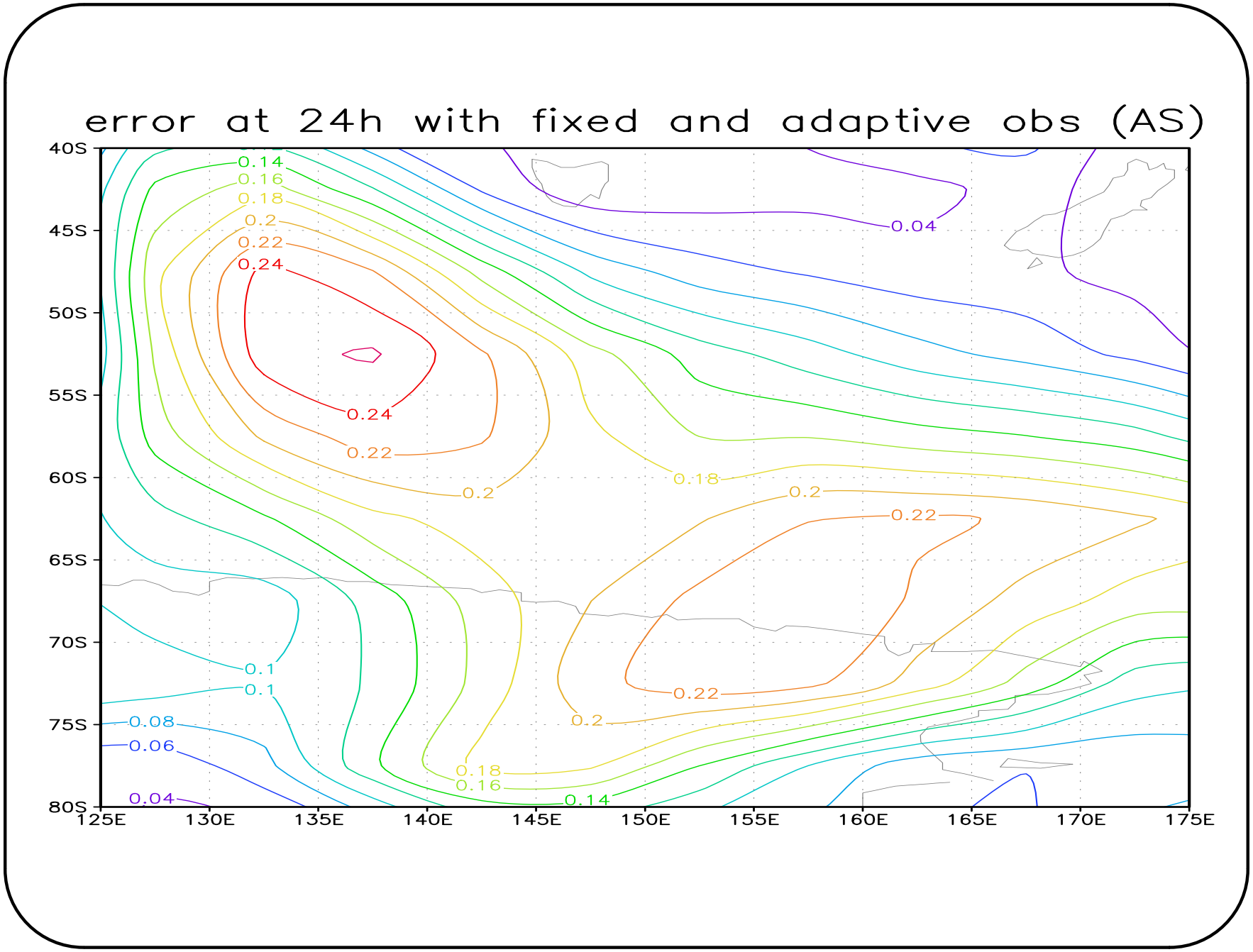
error at 24h with fixed and adaptive obs (AS)
40S
45S
50S
55S
60S
65S
70S
75S
80S
125E
130E
135E
140E
145E
150E
155E
160E
165E
170E
175E
0.14
0.16
0.18
0.2
0.22
0.24
0.04
0.1
0.08
0.06

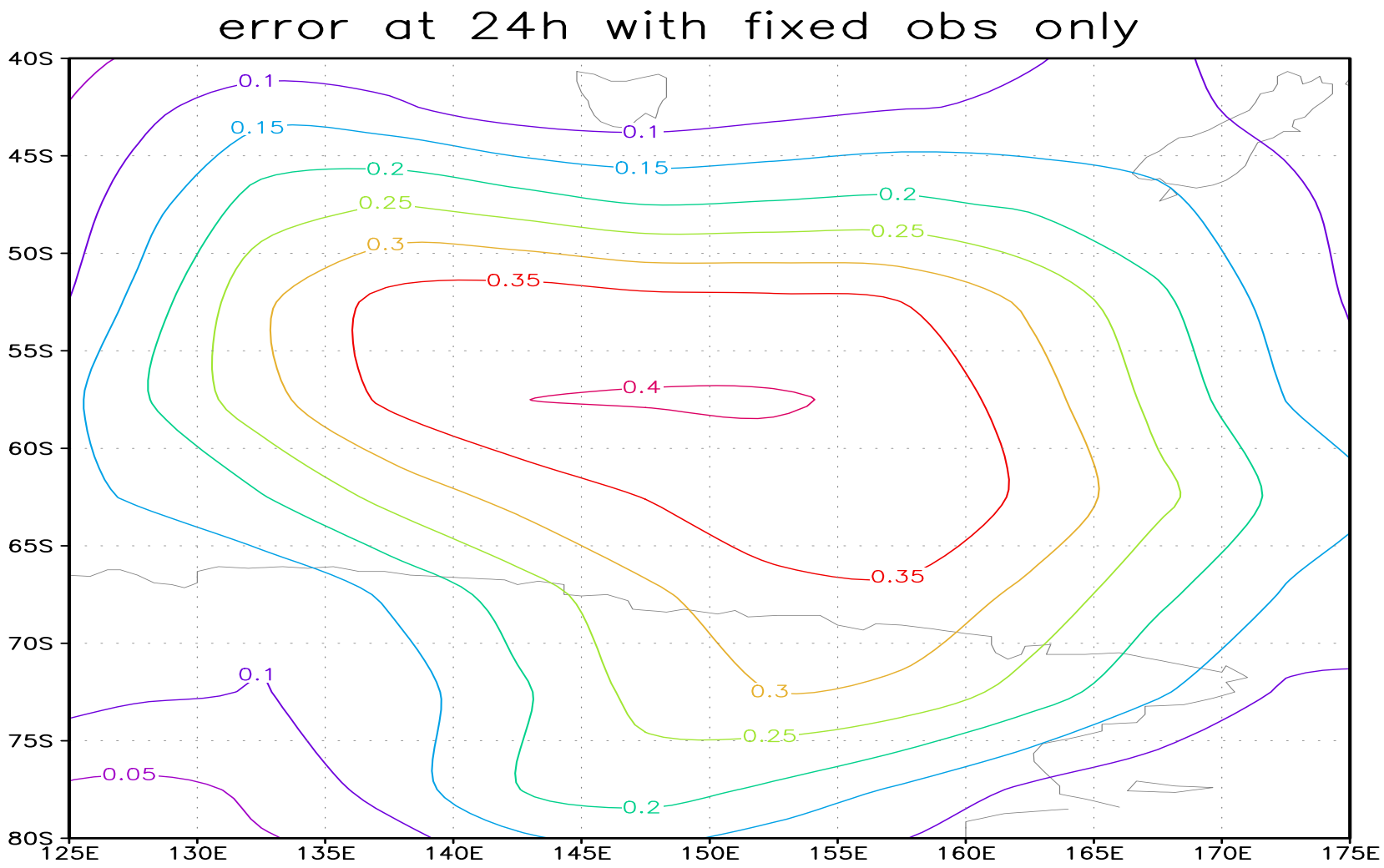
error at 24h with fixed obs only
40S
45S
50S
55S
60S
65S
70S
75S
80S
125E
130E
135E
140E
145E
150E
155E
160E
165E
170E
175E
0.1
0.15
0.2
0.25
0.3
0.35
0.4
0.05

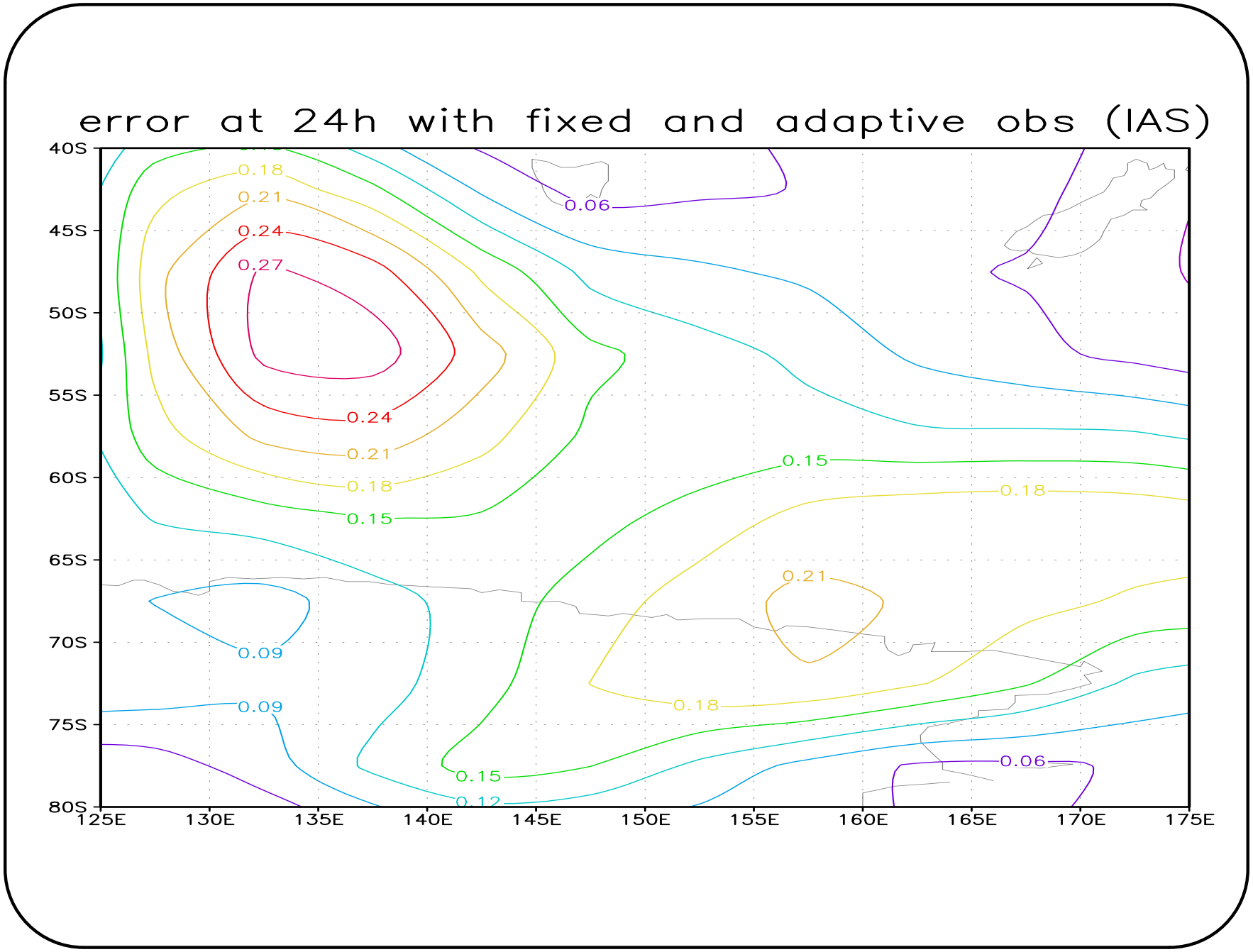
error at 24h with fixed and adaptive obs (IAS)
40S
45S
50S
55S
60S
65S
70S
75S
80S
125E
130E
135E
140E
145E
150E
155E
160E
165E
170E
175E
0.18
0.21
0.24
0.27
0.06
0.24
0.21
0.18
0.15
0.15
0.18
0.21
0.09
0.09
0.18
0.15
0.12
0.06

error of 24h forecast with routine and adaptive obs (IAS)

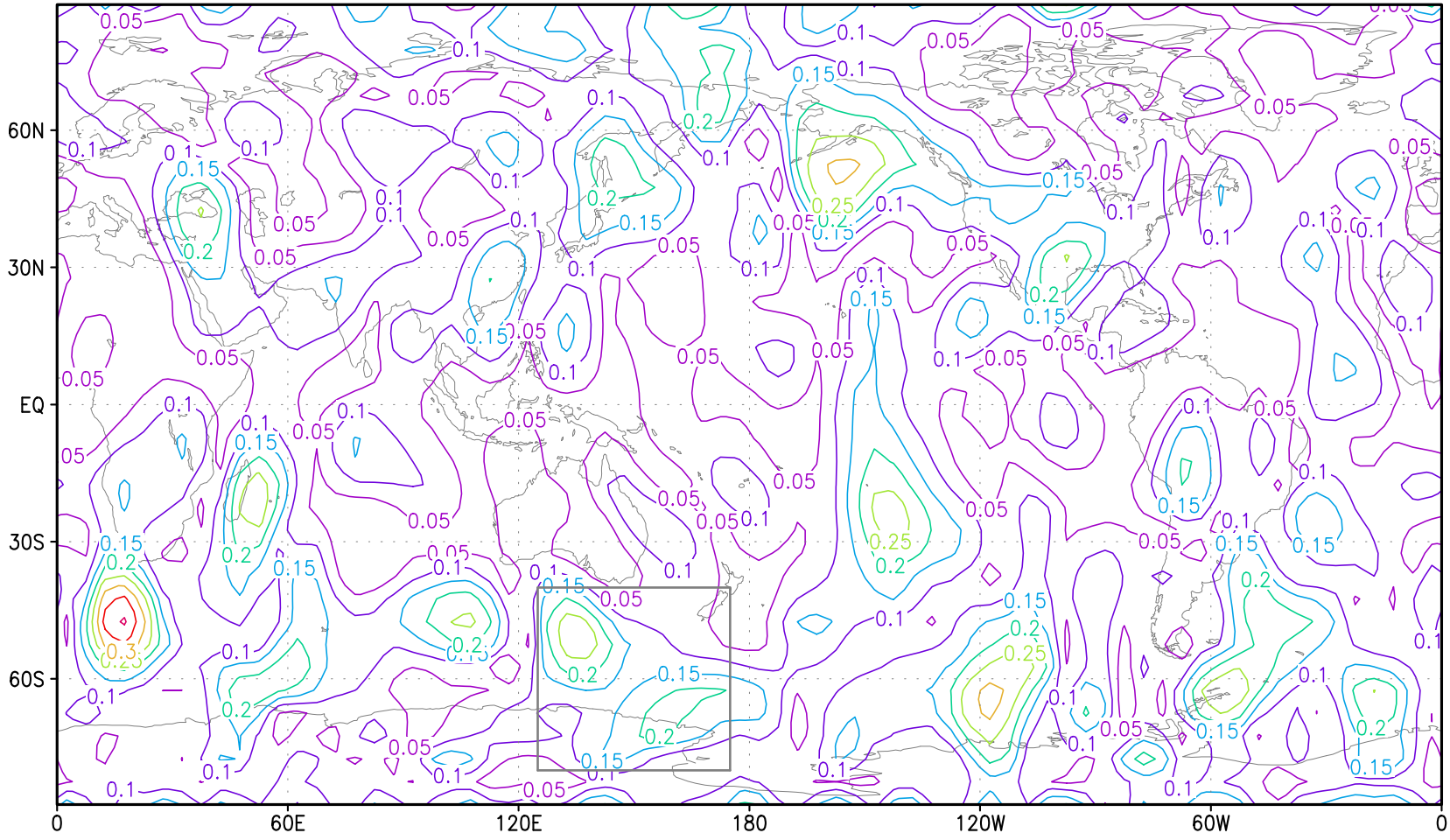

Conclusions and future work

A comparative analysis of adaptive observations strategies using singular vectors and gradient sensitivity techniques was performed in the 4D-Var data assimilation context with a global 2D non-linear shallow water model.

A new adjoint sensitivity approach for targeting observations is proposed which takes into consideration the interaction between the adaptive and fixed location observations.

Preliminary experiments show that the new method offers promising results and its implementation is feasible for large scale models.

Future research directions include

- Implementation and testing on comprehensive operational atmospheric models
- Interaction between adaptive observations and the background estimate (Baker and Daley, QJRMS 2000) in the 4D-Var context.

Singular vectors identify directions in phase space which provide the maximum growth over a finite period in time with respect to specified norms.

Several techniques have been put forward to identify optimal sites for additional observations. Adjoint based techniques such as sensitivity to initial conditions and singular vectors (have been proposed) have been tested for such tasks by many groups of researchers.

As summarized by Langland (2006) targeted observing is a process in which supplementary atmospheric observations are assimilated to improve analyses in selected regions of the atmosphere, and reduce the uncertainty in forecasts of weather events that have large societal or economic impact.

Initial efforts were carried out by Lorenz and Emanuel (1998), Berliner et al. (1999), Barkmeijer et al. (1998), Leutbecher (2003), Langland et al. (1999), Pu and Kalnay (1999) , Morss et al. (2001), Baker and Daley (2000). It has become evident through the work of Barkmeijer et al. (1998, 1999) that use of Hessian singular vectors HSVs) where the Hessian of the cost function (if the background error and observation errors are uncorrelated) is equal to the inverse of the analysis error covariance matrix (Rabier and Courtier 1992, Fisher and Courtier 1995) holds promise for improving adaptive targeting observations.

A methodology of interactive adaptive observations distributed in both time and space was introduced by Daescu and Carmichael (2003) and Daescu and Navon (2004) while the impact of data interaction on targeted observations with a 4-D Var data assimilation and forecast system was presented by Daescu et al. (2006). See also the relevant work of Bergot and Doerenbecher (2002), Bergot (2001), Buizza and Montani (1999), Palmer et al. (1998), Langland and Baker (2004) and Langland (2005).

The advantage of using HSVs (apart from the overhead to have to solve a generalized eigenvalue problem) is that initial time HSVs evolve into leading vectors of the propagated analysis error covariance at verification time.

Barkmeijer et al. (1998, 1999) have shown that the Hessian of the cost function in a variational data assimilation scheme can be used to compute SVs that incorporate an estimate of the full analysis error covariance at initial time. The resulting SVs, referred to as Hessian SVs or (HSVs), are consistent with the data assimilation scheme used to construct the forecast initial conditions. The HSVs also reflect the background and observational error correlations assumed by the data assimilation scheme (Gelaro et al. 2002).

The computational cost of obtaining the HSVs is several times greater than that of the TESVs, since they require solving a generalized eigenvalue problem (Davidson 1975), which precludes the use of the Lanczos algorithm. For a complete survey of second order methods in data assimilation see Le Dimet et al. (2002). In the present paper we present a comparison of TESVs and HSVs for observation targeting using a global shallow-water equations (SWE) model. See Lin and Rood (1997), Lin and Rood (1996), Lin et al. (1994) and Lin (2004) as well as Akella and Navon (2006).

The paper plan is the following.

In section 2 a brief description of the fvSW global model is provided along with the first and second order adjoint required for the HSV research. The generalized Jacobi-Davidson algorithm and its application in the frame work of the JDQZ package as developed by Sleijpen et al. (1996) and Bai, Sleijpen and Van der Vorst (1999) is briefly described in section 3.

In section 4 we review the application of TESV and HSV methods for targeting observations and describe the scenarios of interaction of fixed and adaptive observations. Detailed numerical results are presented in section 5 looking at the differences between HSVs and TESVs in a framework of adaptive observations targeting. Discussion of results of similarity index between TESVs and HSVs is presented in section 6. Conclusions and summary along with further research directions are presented in Section 7.